Benign and Malignant Epithelial Tumors: Lesions of Cutaneous (Skin) Origin

BENIGN AND MALIGNANT EPITHELIAL TUMORS: LESIONS OF CUTANEOUS (SKIN) ORIGIN

ANTHONY A. MANCUSO

KEY POINTS

- Skin cancer is usually not life threatening but can be if more advanced lesions are not evaluated properly before definitive treatment plans are chosen.
- Imaging contributes most in these patients by showing the local extent of tumor, especially with regard to bone invasion, detecting and quantifying perineural spread, and to a lesser extent looking for regional lymph node spread.

The vast majority of all skin carcinoma occurs in the head and neck region. Sun exposure is the major etiologic factor. There is a lower incidence in dark-skinned races compared to those with lighter complexions.1,2 The rate of occurrence and aggressiveness of skin cancer increases in immune-compromised patients. Toxic exposures and hereditary disorders can also predispose patients to this risk.

The critical anatomy in evaluating skin cancer relates the skin to the subcutaneous fat and that deeper fat beneath the superficial musculoaponeurotic system (SMAS) of the face. The SMAS is the facial equivalent of the superficial fascia in the neck. The fat deep to the SMAS and its relationship to the neurovascular bundles of the face is critical knowledge for evaluating imaging studies of patients with advanced skin cancer. The relationships are particularly important with reference to the distal branches of the facial nerve and all three divisions of the trigeminal nerve, as discussed in Chapter 21. The more proximal course of V1, V2, and V3, as well as that of the facial nerve, must also be completely understood to assure the best medical decision making (Figs. 21.9, 21.10, 21.50–21.52, and 24.1–24.9).

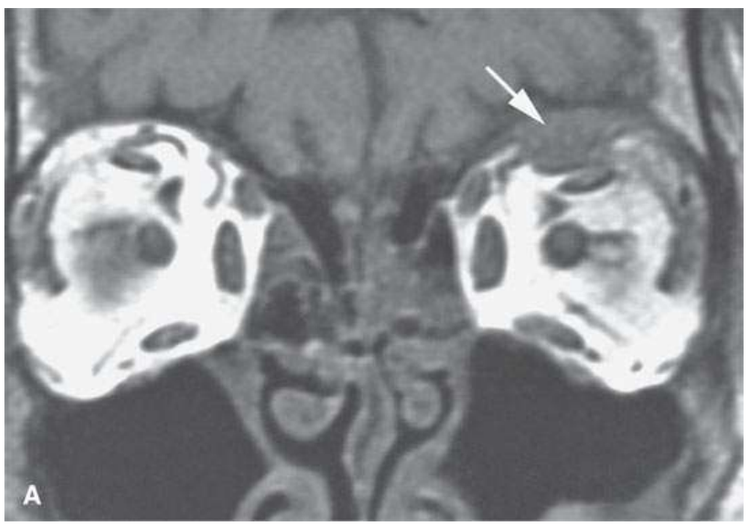

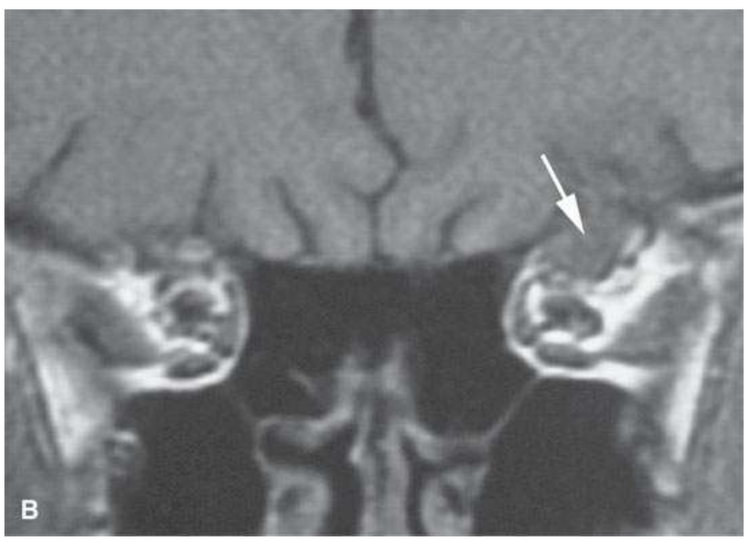

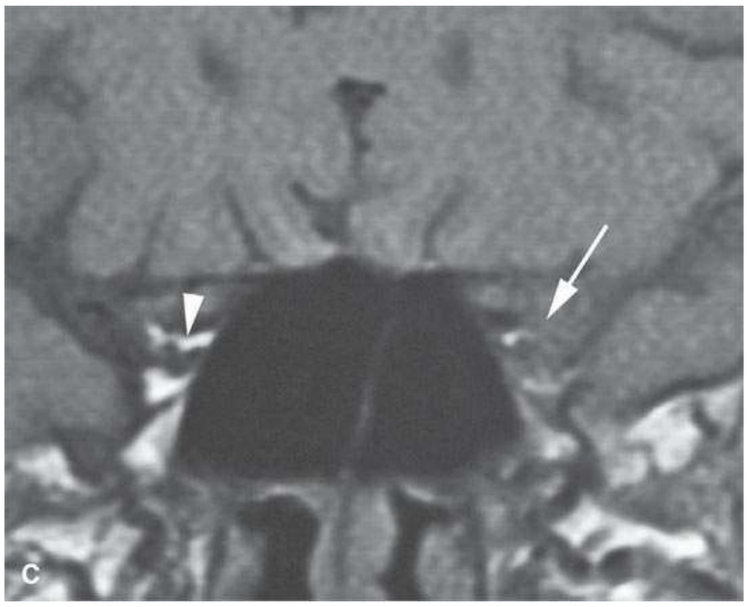

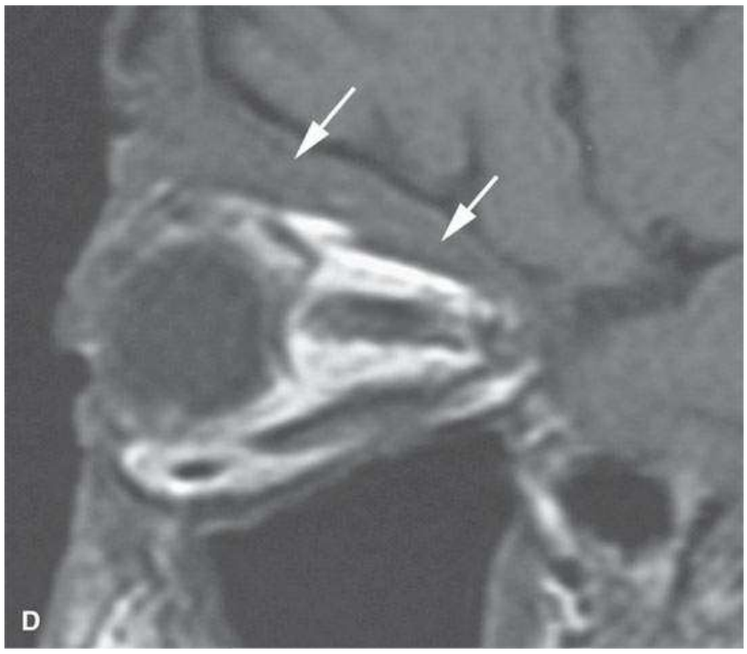

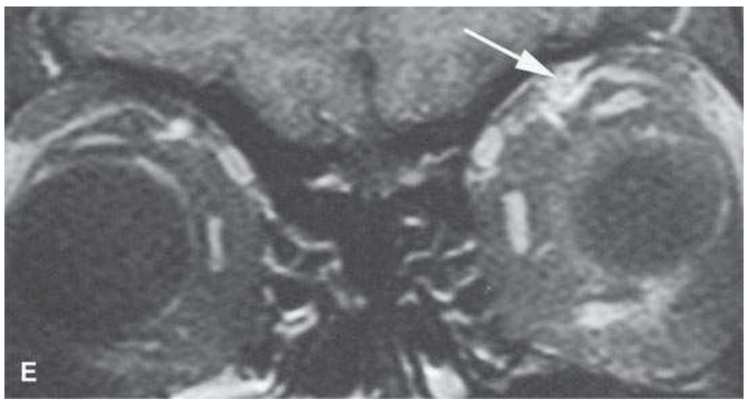

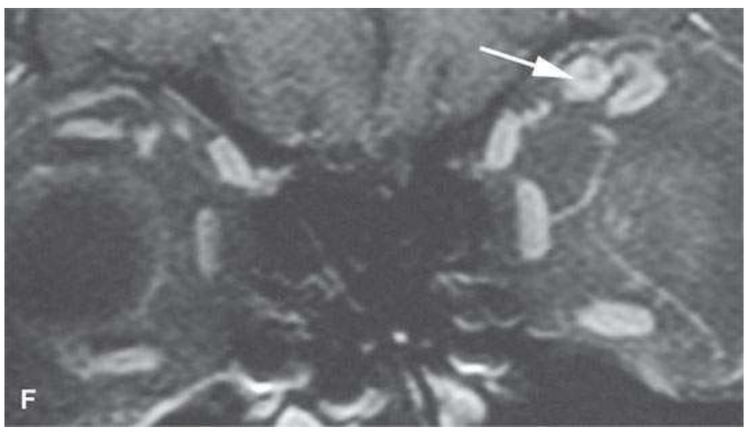

FIGURE 24.1. Magnetic resonance imaging of a patient with perineural spread of forehead squamous cell carcinoma along the first division of the trigeminal nerve to the orbital apex and superior orbital fissure. **A–D**: Non–contrast-enhanced T1-weighted (T1W) images show the typical location of such spread superior and medial in the orbit along the supratrochlear and supraorbital neurovascular bundles. **D—F**: Contrast-enhanced T1W fat-suppressed images.

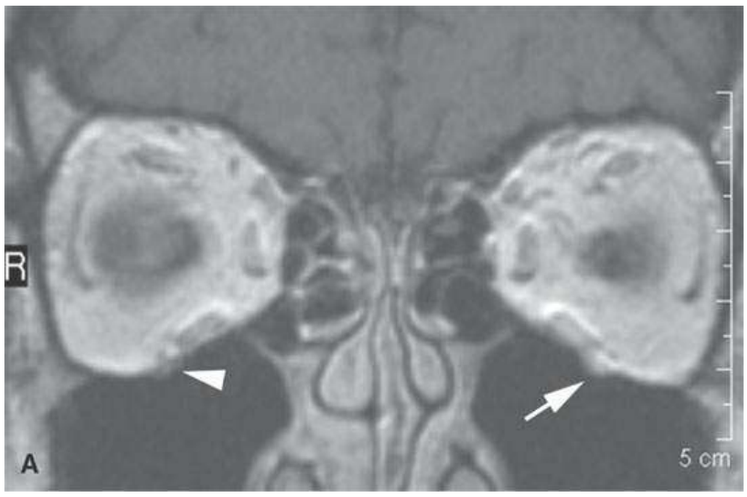
R
A
5 cm

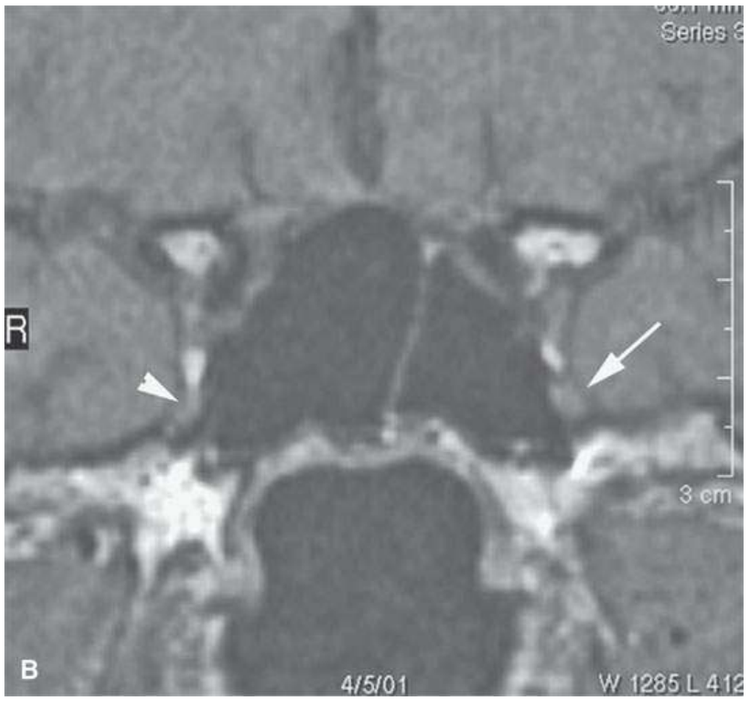
R
3 cm
B
4/5/01

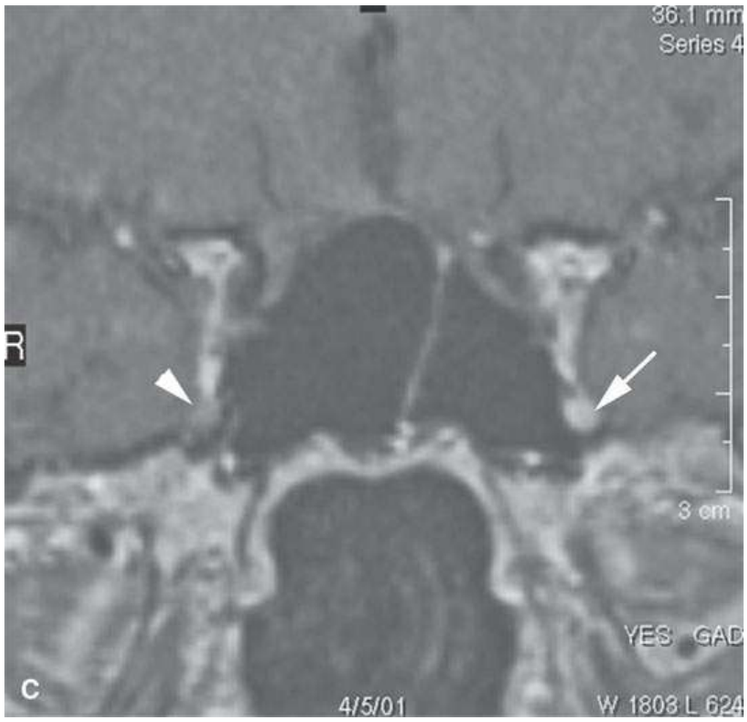
36.1 mm
R
3 cm
C
4/5/01

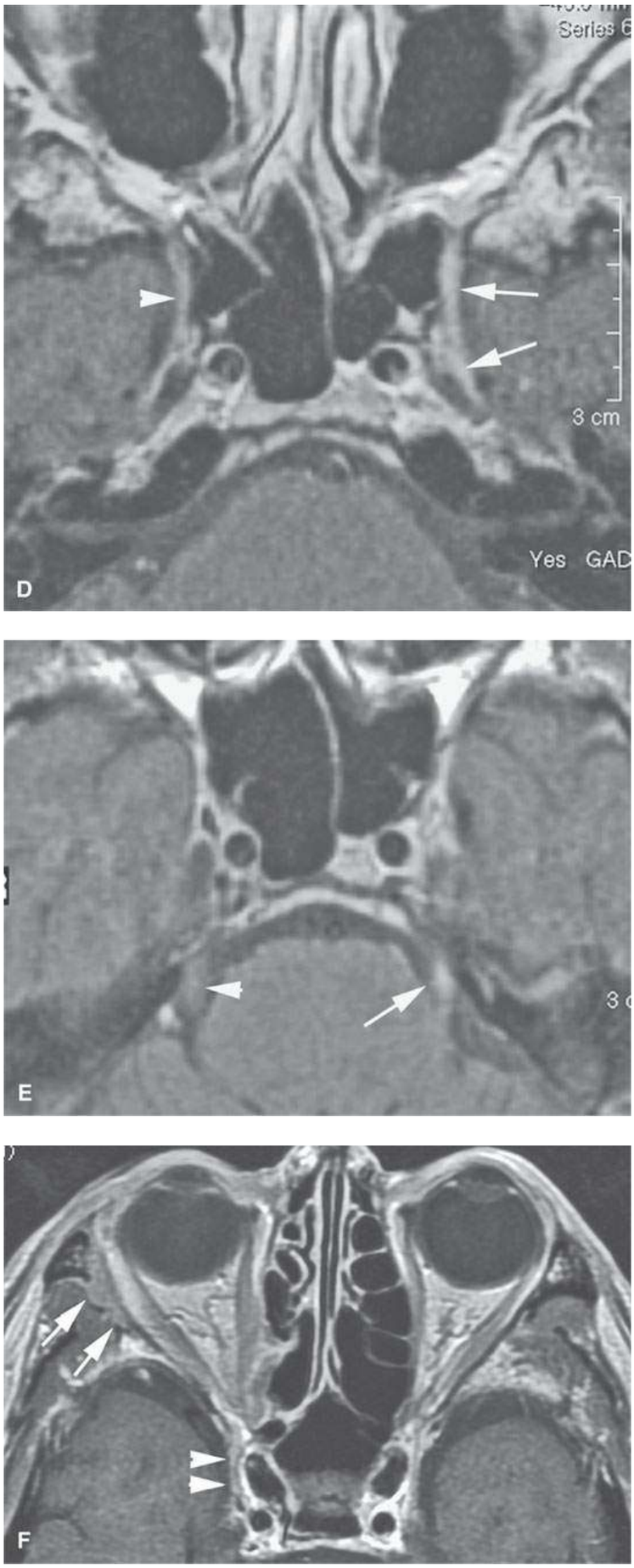

FIGURE 24.2. Contrast-enhanced T1-weighted (T1W) magnetic resonance imaging (MRI) of a patient with perineural spread of squamous cell carcinoma (SCCA) of the nasolabial fold region along the second division of the trigeminal nerve to the trigeminal nerve cisternal segment; the involved nerve is enlarged and enhances abnormally *(arrows)* compared to the normal nerve *(arrowheads)* in all of its segments **(A–E). F:** Contrast-enhanced T1W MRI of another patient with perineural spread of facial skin SCCA along the frontozygomatic branch of V2 *(arrows)* and the foramen rotundum *(arrowheads)***.**

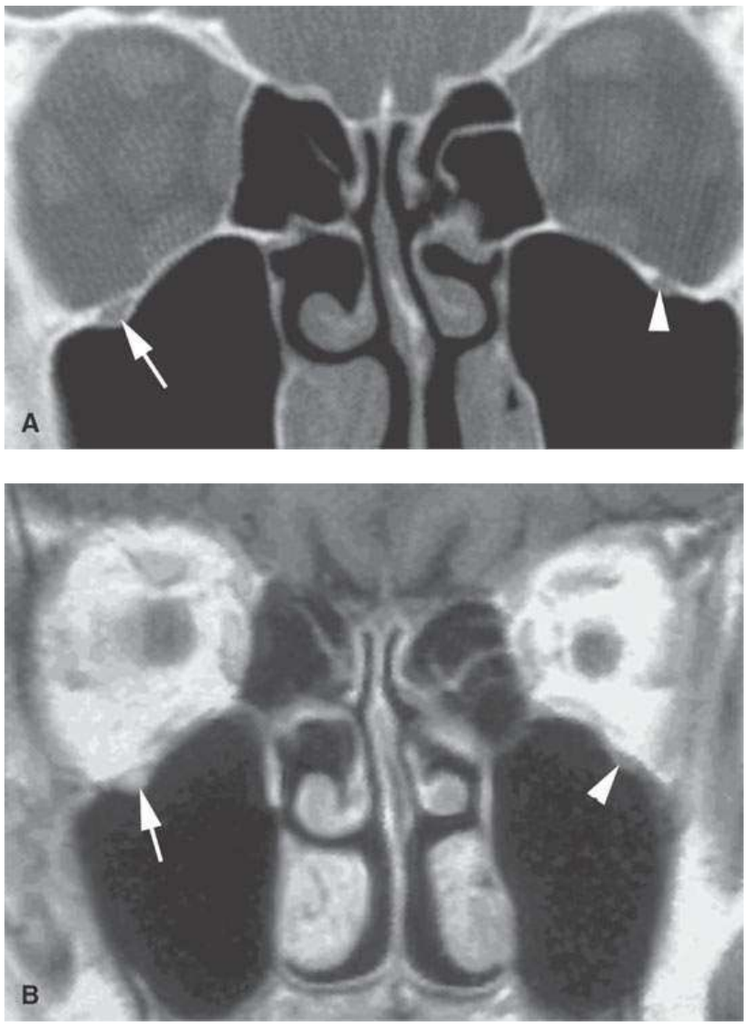

FIGURE 24.3. A patient with squamous cell carcinoma of the cheek spread along V2 and limited to the infraorbital canal. The disease was controlled with radiotherapy that spared the eye**. A**: Computed tomography showing the slightly enlarged bony infraorbital canal *(arrow)* compared to the normal side *(arrowhead)***. B**: Contrast-enhanced T1-weighte image showing V2 to be enlarged and abnormally enhancing *(arrows)* compared to the normal side *(arrowheads)***.**

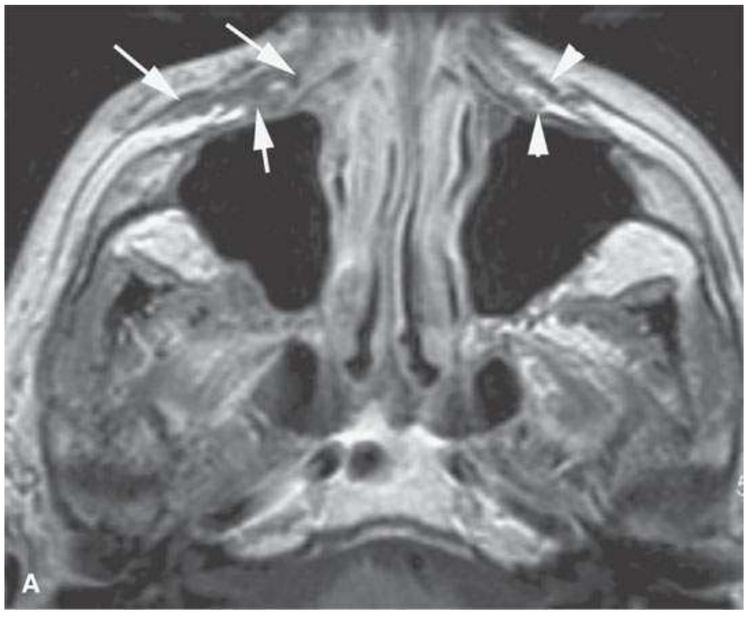

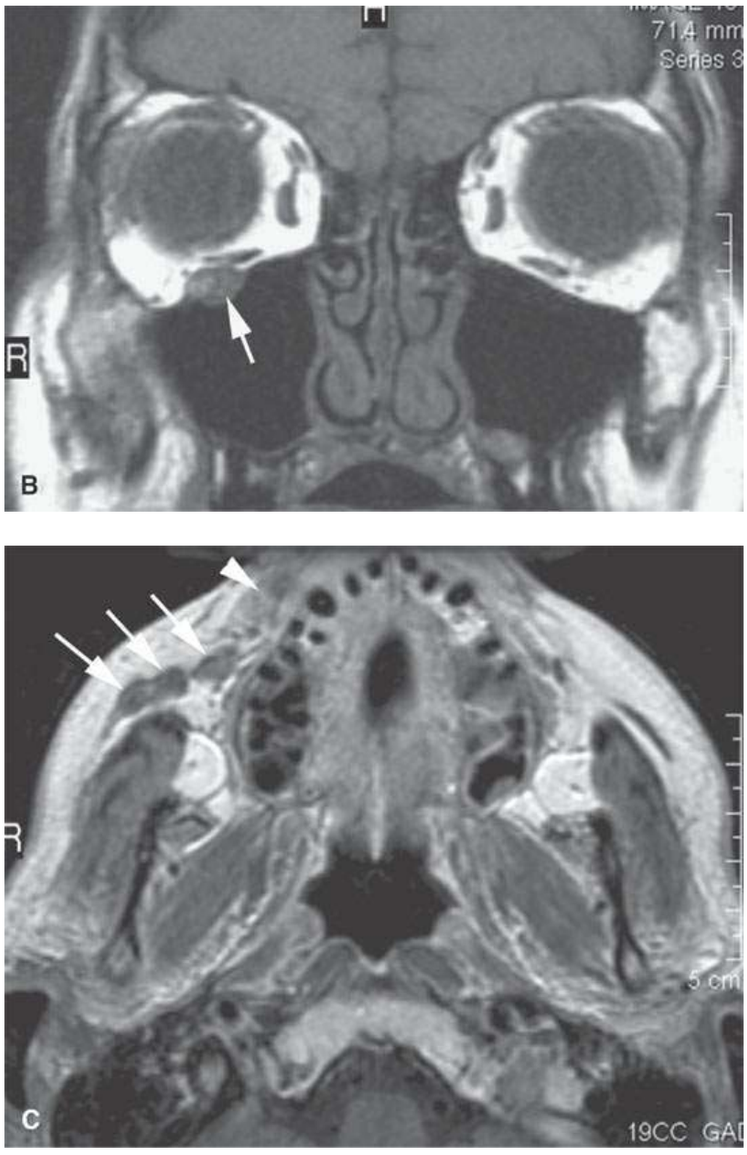

FIGURE 24.4. Contrast-enhanced T1-weighted images in a patient with squamous cell carcinoma spread of the cheek along V2 and the buccal branch of the facial nerve. **A:** There is thickening along and deep to the superficial musculoaponeurotic system (SMAS) *(arrows)* and enlargement of the distal branches of the infraorbital nerve deep to the SMAS *(arrows)* compared to the normal side *(arrowheads)*. **B:** The infraorbital nerve is enlarged and enhances abnormally *(arrow)*. **C:** There is thickening of the SMAS along the upper lip *(arrowhead)* and nodular enlargement of the distal branches of the buccal branch of the facial nerve *(arrows)* compared to the normal side.

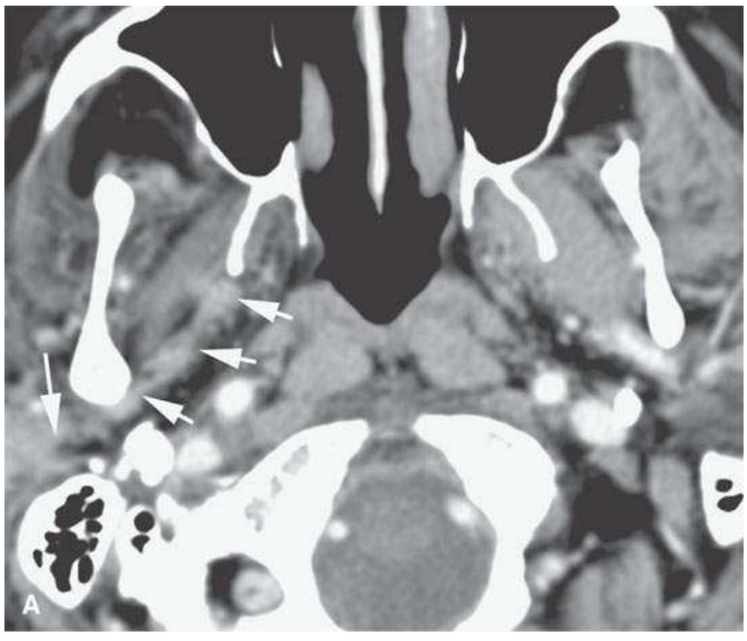

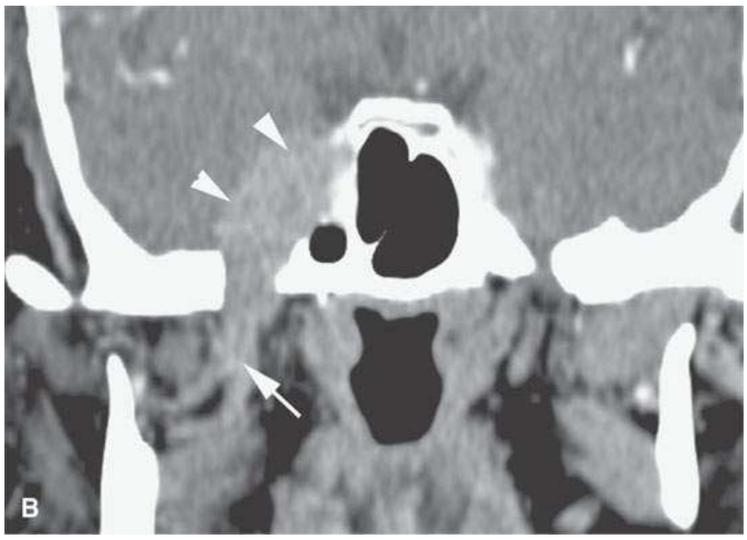
B

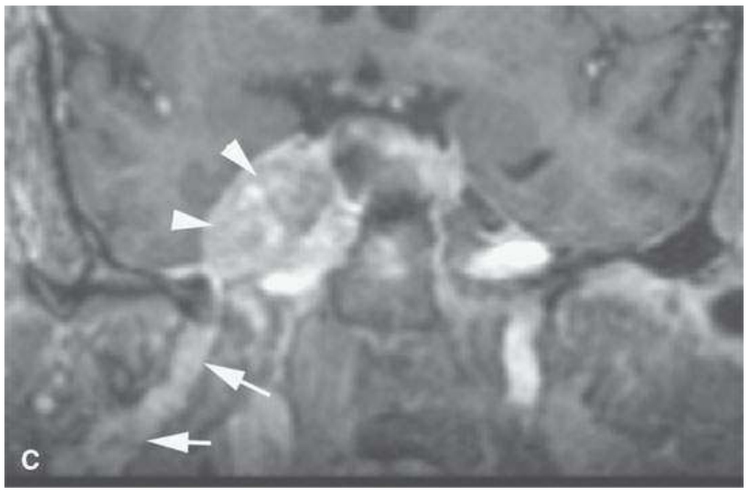
C

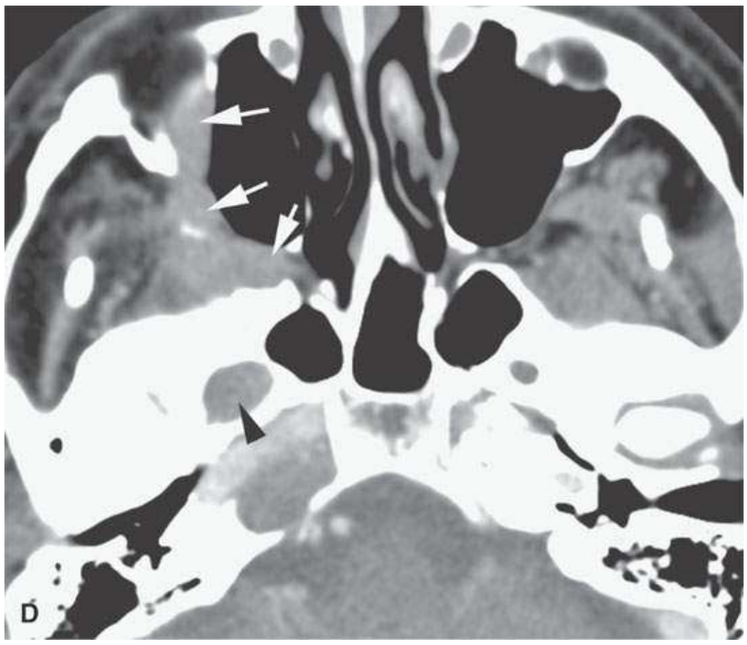
D

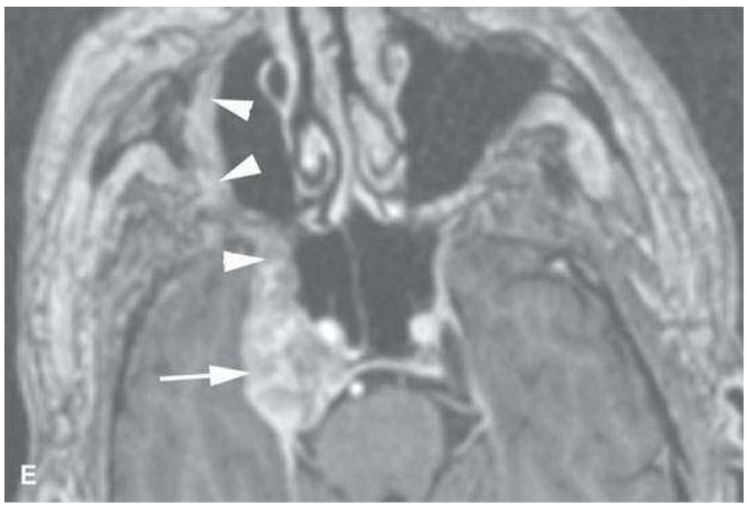
E

FIGURE 24.5. A patient with melanoma of the periauricular region spread along V3 to the trigeminal ganglion proximally**. A:** Contrast-enhanced computed tomography (CT) showing spread from the auriculotemporal nerve *(arrow*) to V3 *(arrowheads)***. B:** Continued spread from the main trunk of V3 in the masticator space *(arrow)* to the trigeminal cistern *(arrowheads)***. C**: Contrast-enhanced T1-weighted (T1W) magnetic resonance (MR) showing trigeminal cistern involvement *(arrowheads)* from V3 spread *(arrows)* to correlate with CT in **(B). D:** Anterograde spread from the trigeminal ganglion to the pterygopalatine fossa and infraorbital nerve *(arrows*) as well as foramen ovale enlargement *(arrowhead)***. E**: Contrast-enhanced T1W MR showing trigeminal cistern involvement *(arrow)* with anterograde V2 spread *(arrowheads)***.**

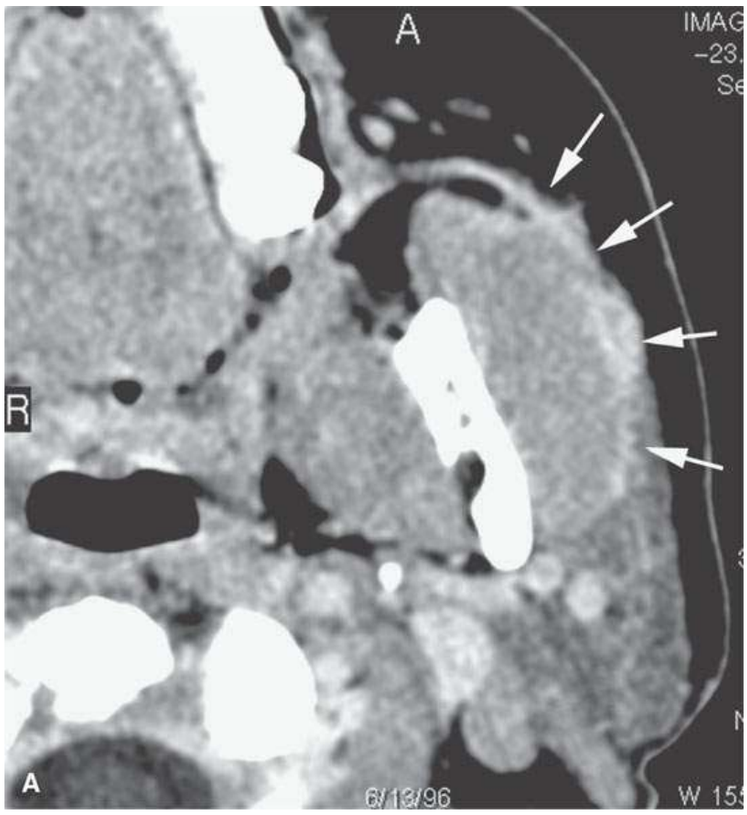

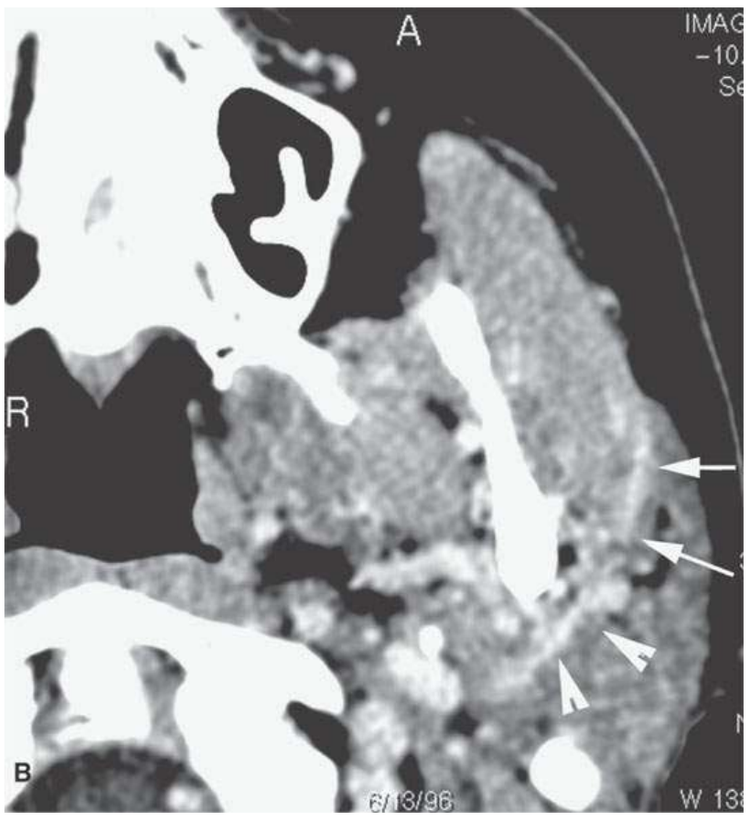

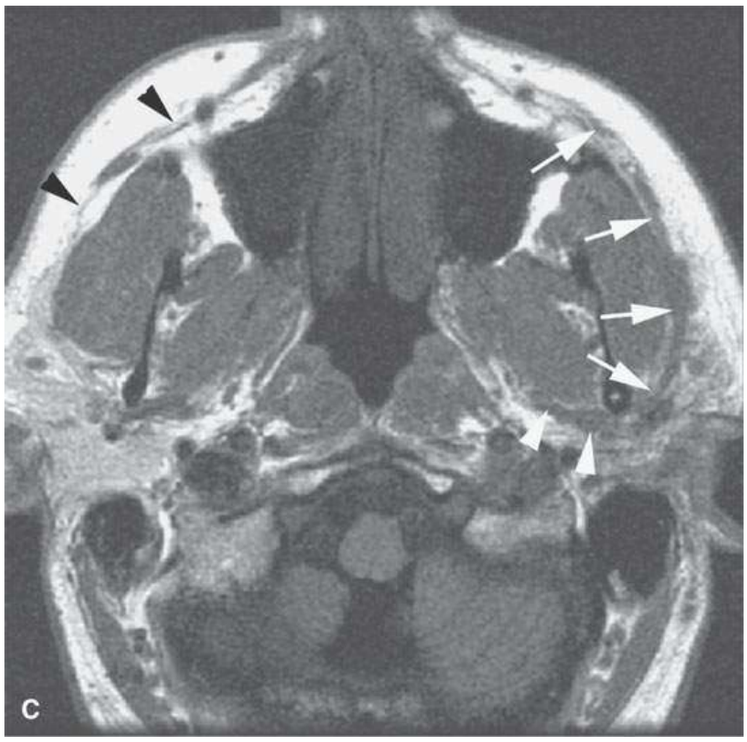
C

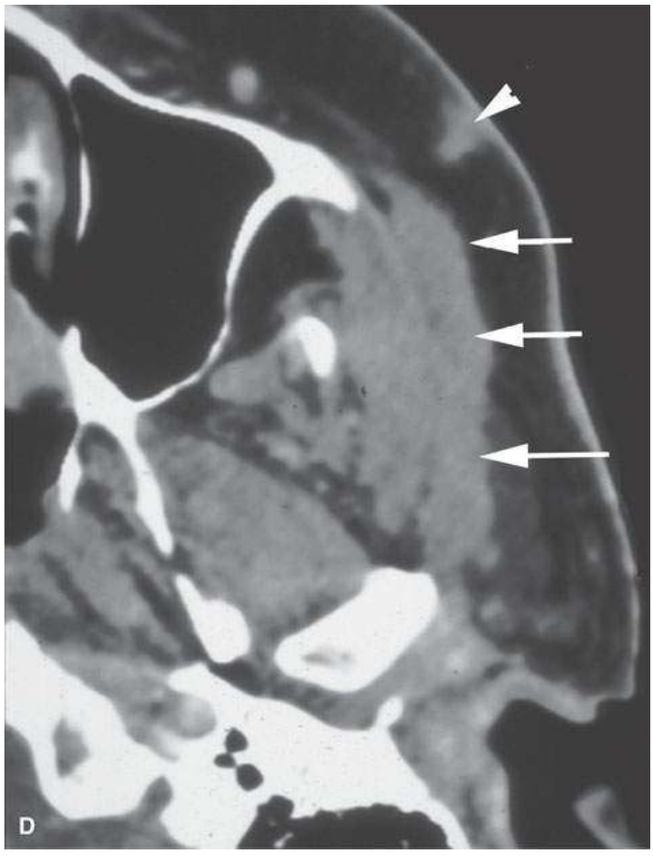
D

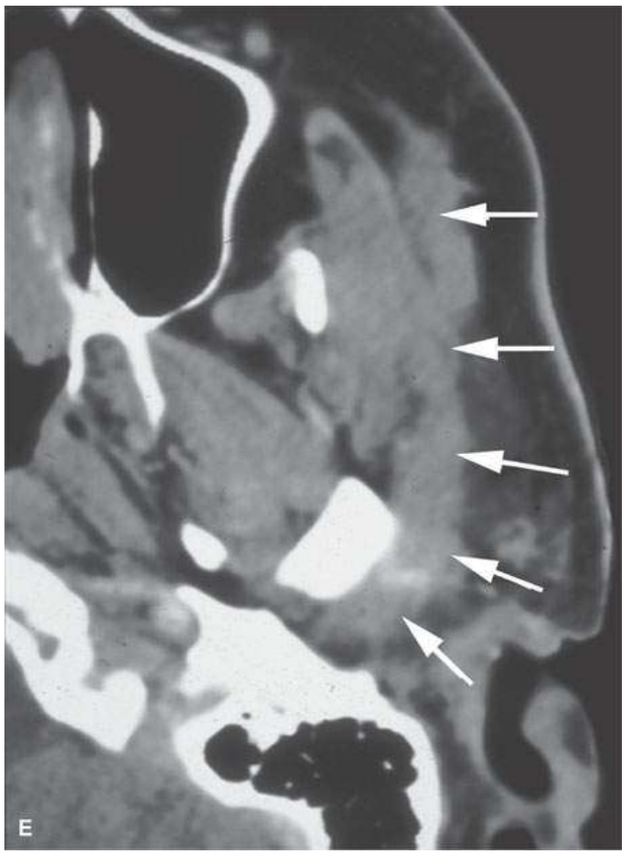

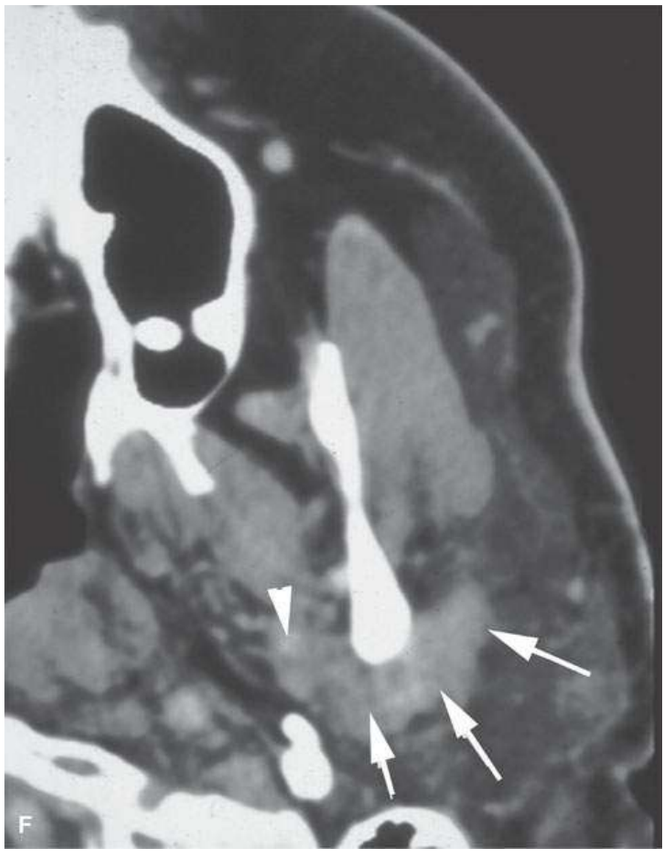

FIGURE 24.6. Patient with squamous cell carcinoma (SCCA) of the cheek with slow onset of peripheral facial nerve palsy. **A, B:** Contrast-enhanced computed tomography (CECT) showing tumor causing enlargement and an abnormal enhancement of the buccal division of the facial nerve back to the main trunk *(arrows)* in **(A)** with continuation **(B)** to the main trunk of the facial nerve *(arrowheads)*. **C:** T1-weighted image for correlation with **(A)** and **(B)** and comparison of normal anatomy on the right where the SMAS is not denervated and infiltrated *(black arrowheads)*. **D–F:** Patient who "picked off" a SCCA of the cheek and presented about 2 years later with slow onset of peripheral facial nerve palsy.CECT showing a subcutaneous nodule of residual tumor **(D)** with perineural tumor causing gross enlargement of the zygomatic division of the facial nerve back to the main trunk *(arrows)* in **(D)** with continuation **(E)** to the main trunk of the facial nerve *(arrows)* and in **(F)** growth along the auriculotemporal nerve to its junction with V3 in the masticator space *(arrowheads)*.

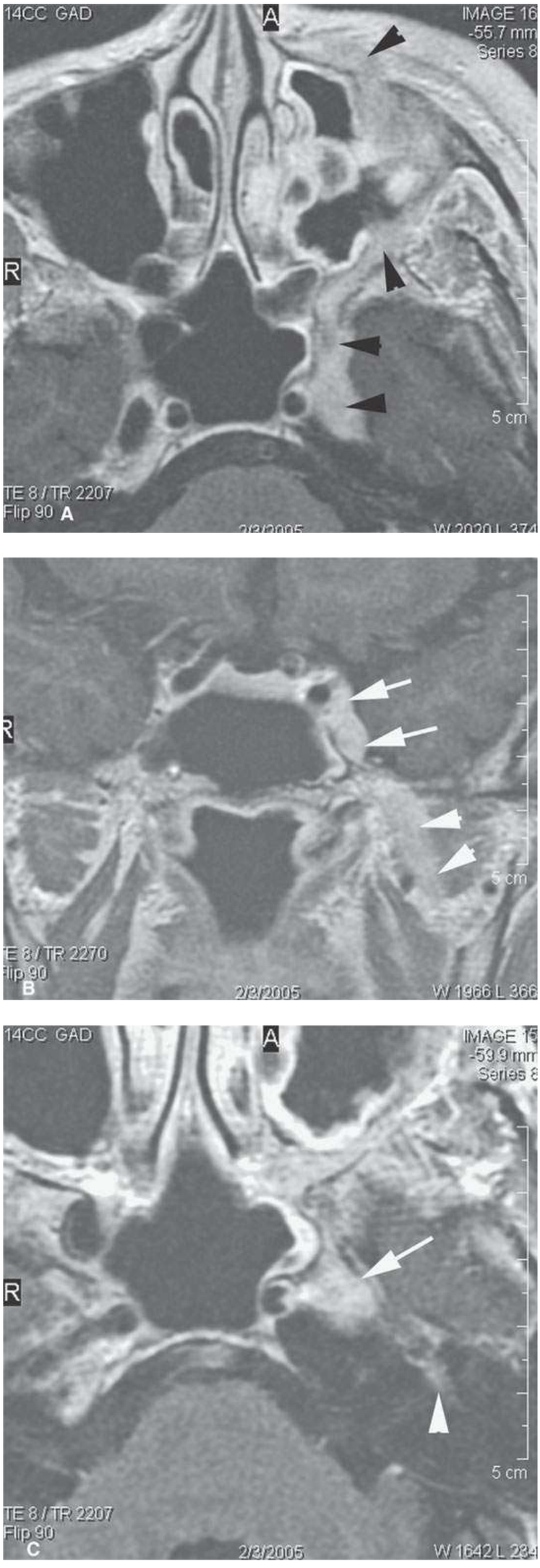

FIGURE 24.7. Contrast-enhanced T1-weighted magnetic resonance imaging of a patient with perineural spread of recurrent basal cell carcinoma of the nasolabial fold and cheek region along the second division of the trigeminal nerve to the trigeminal ganglion and cistern proximally, where it spreads to the first genu of the facial nerve via the petrosal nerve**.** The involved nerves are enlarged and enhance abnormally**. A:** Tumor infiltrates from the distal ramifications of the infraorbital nerve beneath the superficial musculoaponeurotic system to the trigeminal ganglion *(arrowheadss*)**. B:** Tumor spreads anterograde from the

ganglion and cistern *(arrows)* to V3 *(arrowheads)*. **C:** Tumor spreads from the ganglion along the petrosal nerve *(arrow)* to the facial nerve anterior genu *(arrowhead)*.

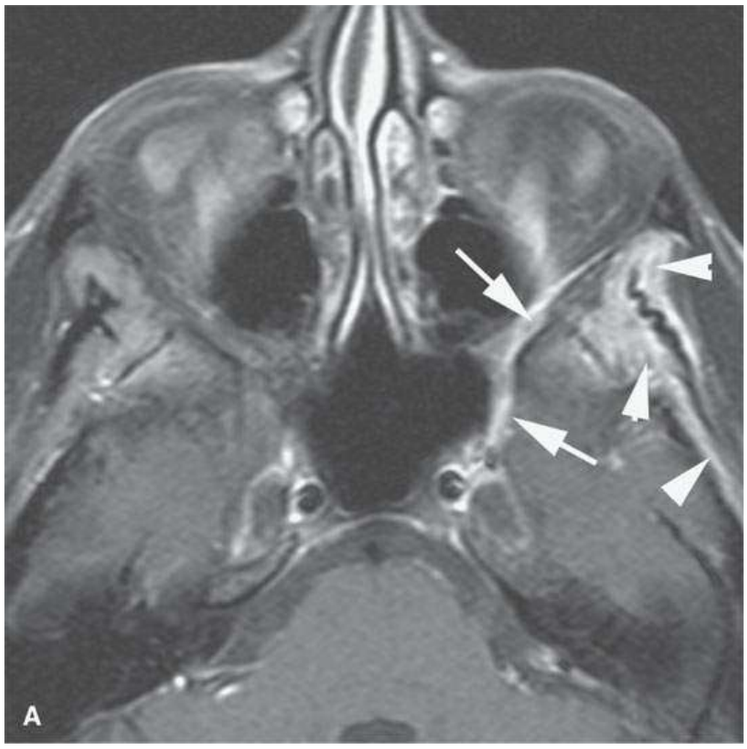

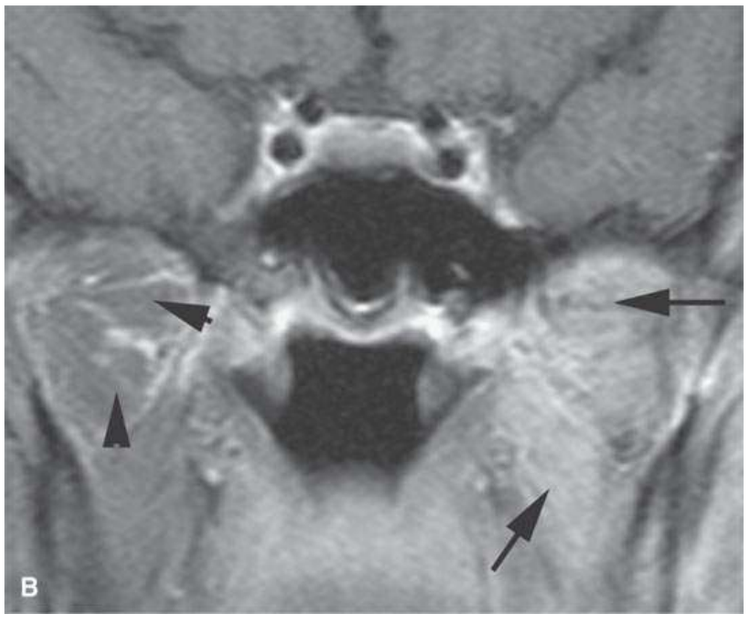

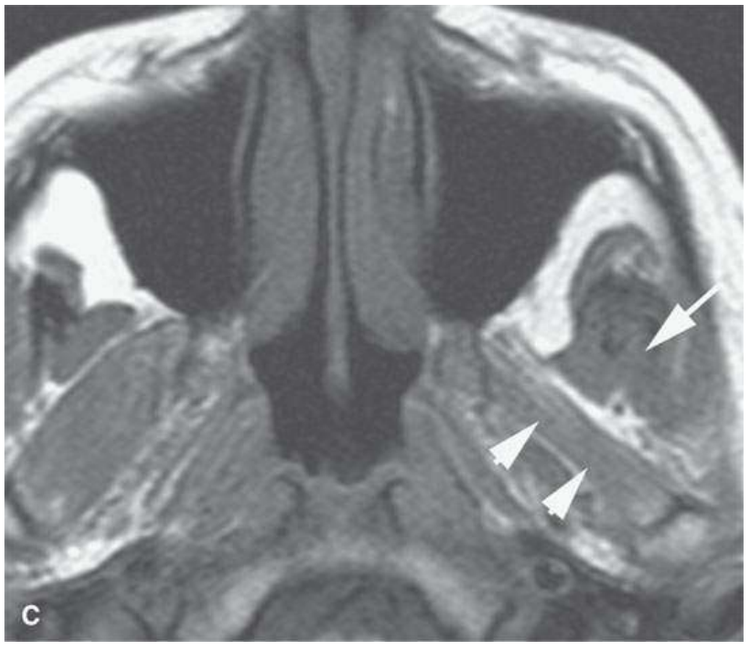

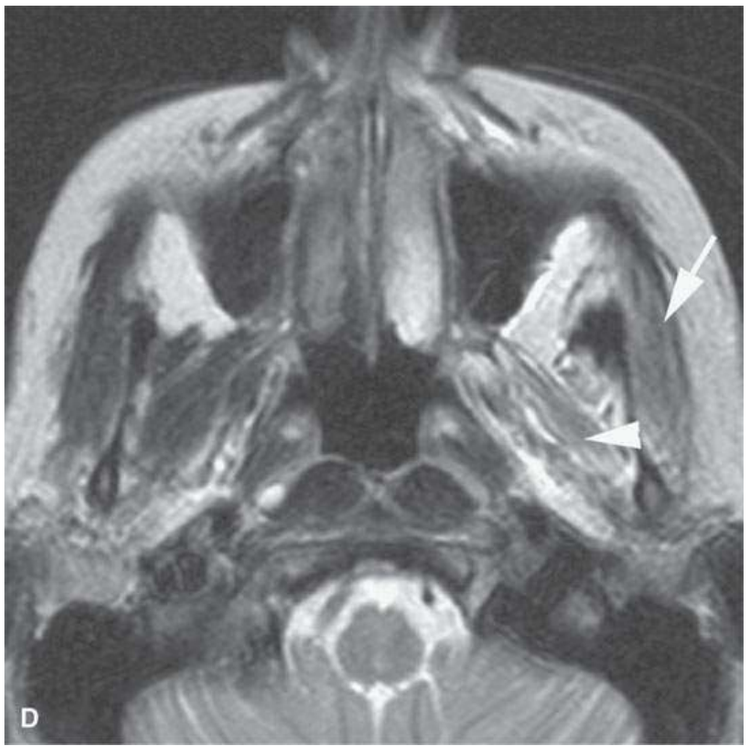

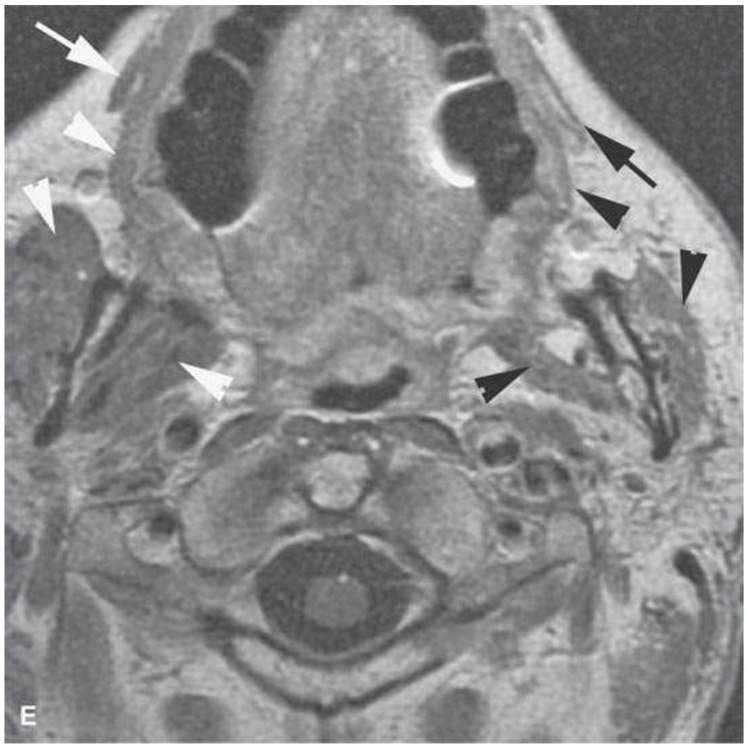

FIGURE 24.8. A patient with squamous cell carcinoma spread of the cheek along V2 illustrating secondary denervation atrophy of the muscles of mastication in a chronic active phase**. A**: Contrast-enhanced fat-suppressed T1-weighted (T1W) images showing the perineural V2 spread *(arrows)* and the enhancement of the denervated temporalis muscle**. B**: Contrast-enhanced fat-suppressed T1W images showing the enhancement of the denervated pterygoid muscles *(arrows)* compared to the normal muscle on the opposite side *(arrowhead)***. C**, **D**: Another patient showing more end-stage denervation atrophy, the pterygoid muscles *(arrowheads)* with diminished bulk, and some early fat replacement, while the temporalis muscle still appears somewhat swollen and edematous*(arrow)***. E**: T1-weighted contrast-enhanced MRI in a third patient showing the effects of both V3 and facial nerve perineural spread of cancer**.** The muscles of facial expression are atrophied on the left *(black arrow)* compared to the normal right side *(white arrow*) and the masseter and pterygoid muscle atrophic on the left *(black arrowheads)* compared to the normal right side *(white arrowheads*)**.**

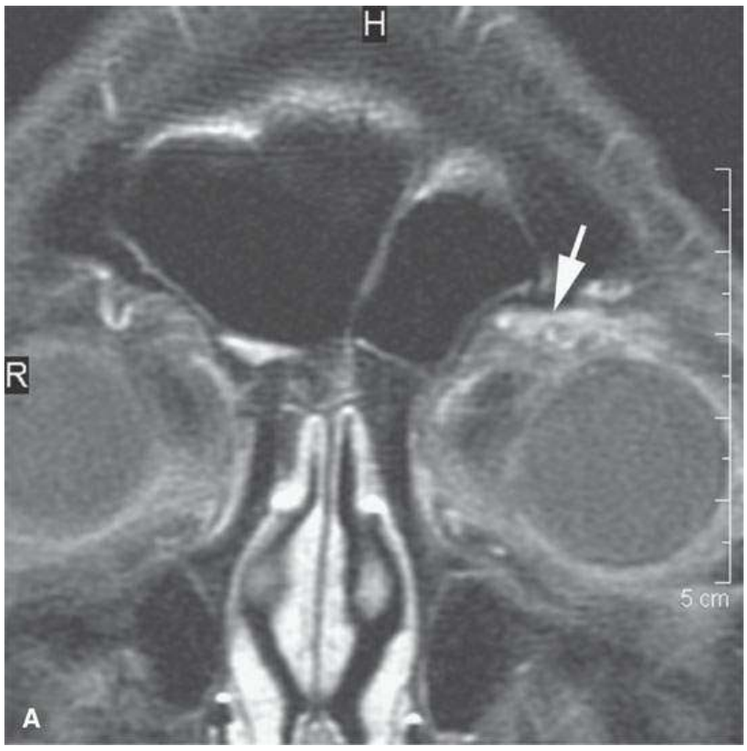
H
R
5 cm
A

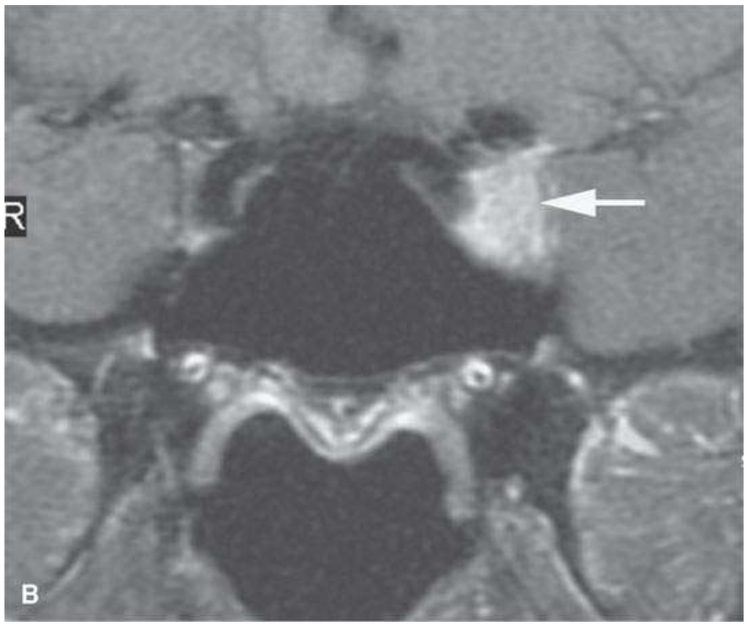
R
B

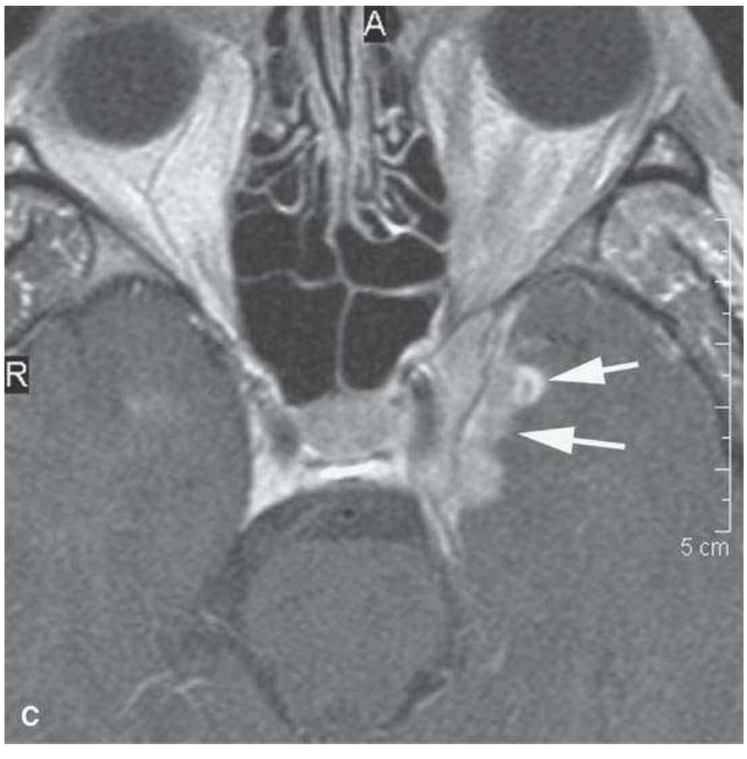
A
R
5 cm
C

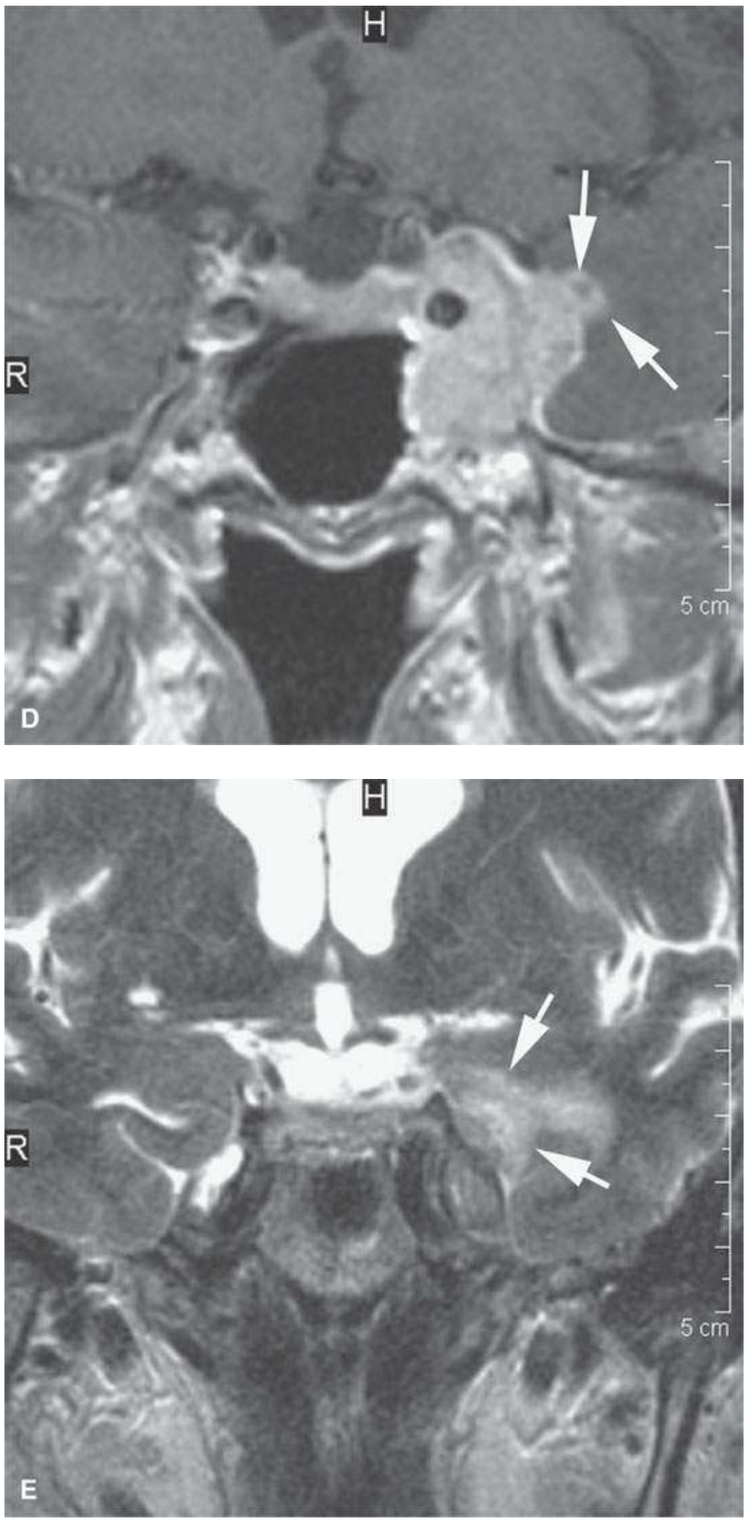

FIGURE 24.9. Magnetic resonance imaging of a patient with perineural spread of forehead squamous cell carcinoma along the first division of the trigeminal nerve to the trigeminal ganglion from which it invades adjacent brain Findings are indicated by *arrows* in each figure. **A–D:** Contrast-enhanced T1-weighted images show the typical location of such spread superior and medial in the orbit along the supratrochlear and supraorbital neurovascular bundles **(A)**, disease at the orbital apex **(B)** and to the trigeminal ganglion and cistern **(C, D)**, where it invades across the lateral dura of the cavernous sinus to invade the brain. **E:** The brain involvement is confirmed by the T2-weighted image showing brain edema.

The anatomy and physiology of lymphatic spread must also be completely understood to most effectively interpret images in patients with skin cancer (Figs. 24.10–24.14). The most superficial lymphatics in the skin are the valveless capillary channels of the dermis. Deeper dermal lymphatic trunks and subcutaneous trunks have valves. The primary lymph nodes for carcinomas of the scalp and face are levels 1A, 1B, 5, those of the parotid region, and the mastoid, occipital and posterior neck nodes, as discussed in Chapters 149 and 157. The less well known facial nodes are also at significant risk. Subsequent drainage of level 1 nodes to level 2 put levels 2, 3, and 4 at secondary risk.

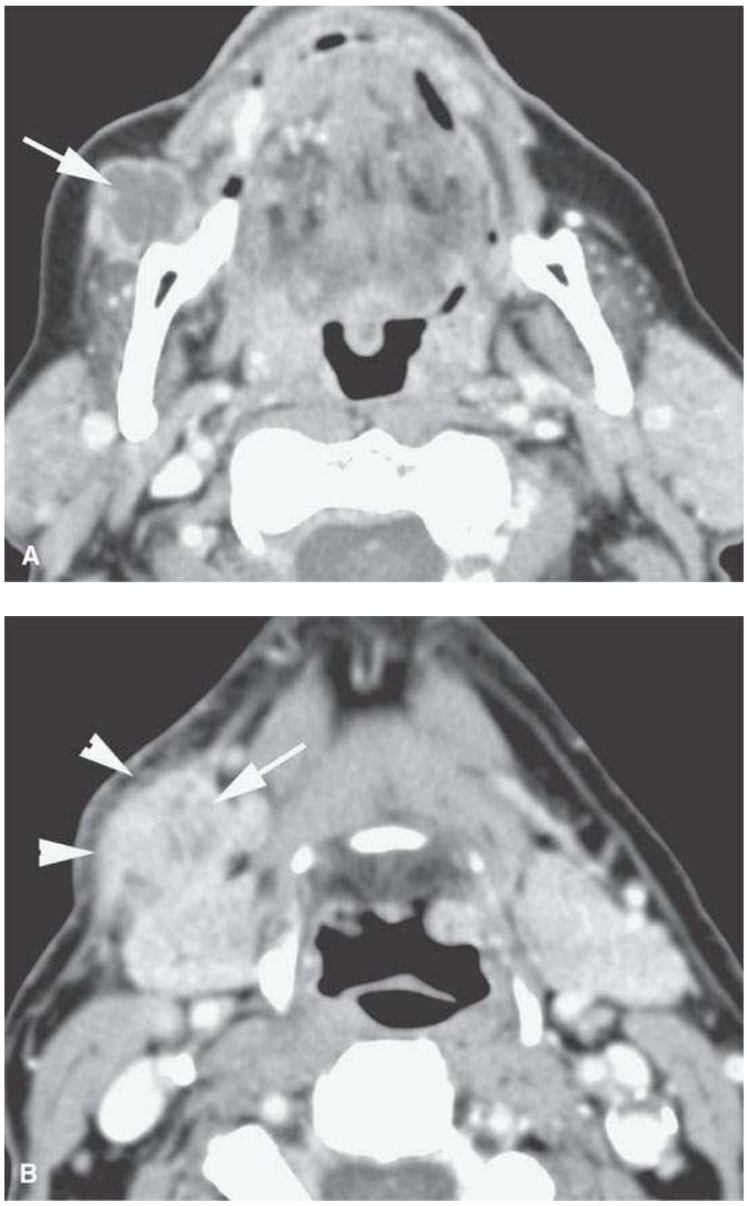

FIGURE 24.10. Contrast-enhanced computed tomography of a patient with squamous cell carcinoma of the cheek with metastatic mandibular node in the facial group (*arrow* in **A**) and more typical nodal involvement of a level 1B node (*arrow* in **B**) with extranodal spread across the superficial musculoaponeurotic system very likely involving the related mandibular division of the facial nerve.

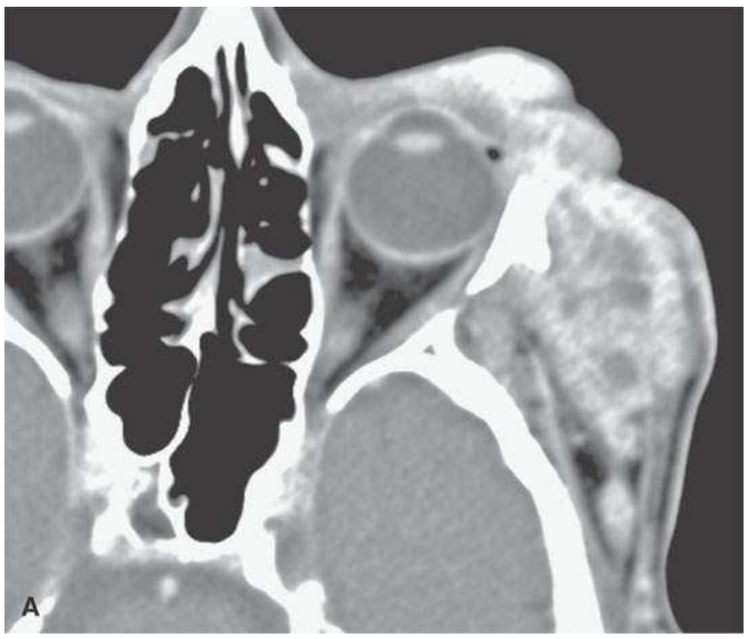

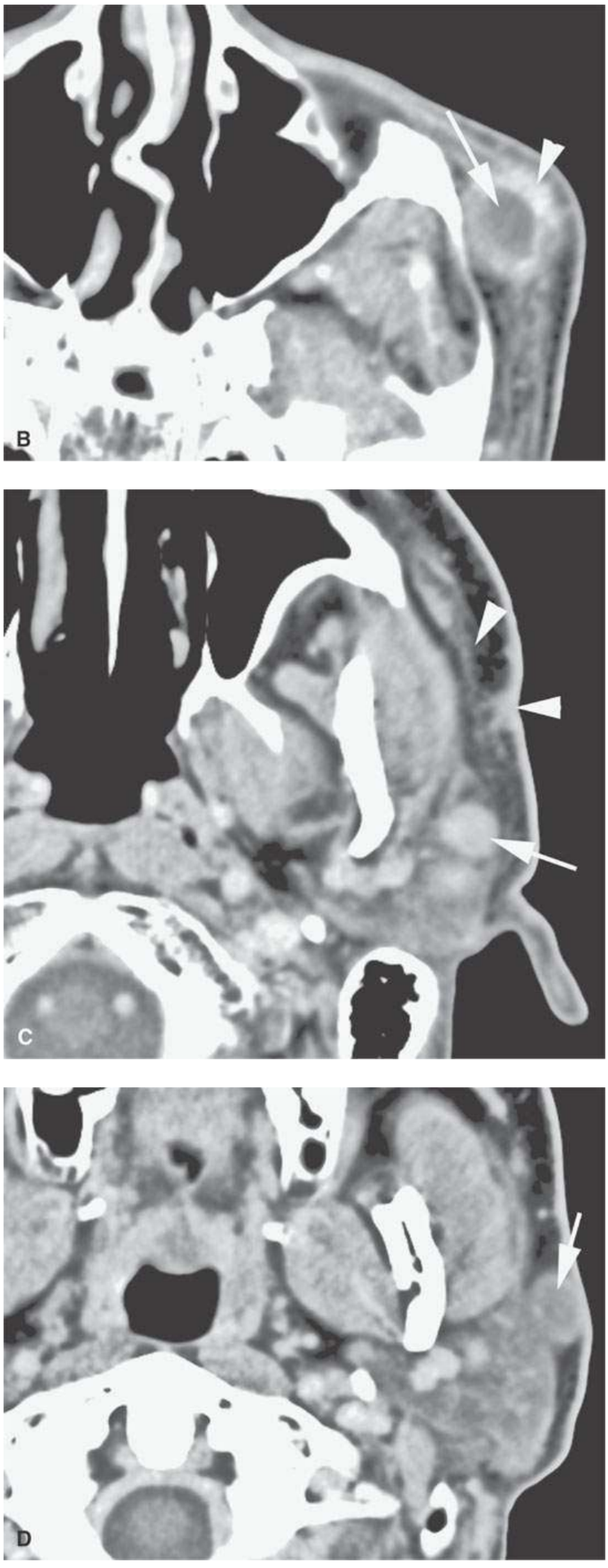

FIGURE 24.11. Contrast-enhanced computed tomography of a patient with extensively recurrent squamous cell carcinoma of the periorbital region **(A)** and in **(B)** a metastatic zygomatic node *(arrow)* of the facial group with early extranodal spread *(arrowhead)*. **C**: There is also spread in the subcutaneous fat and along the superficial musculoaponeurotic system *SMAS (arrowheads)* suggestive of lymphatic obstruction with metastatic parotid nodes *(arrows)* both within **(C)** and outside **(D)** the gland.

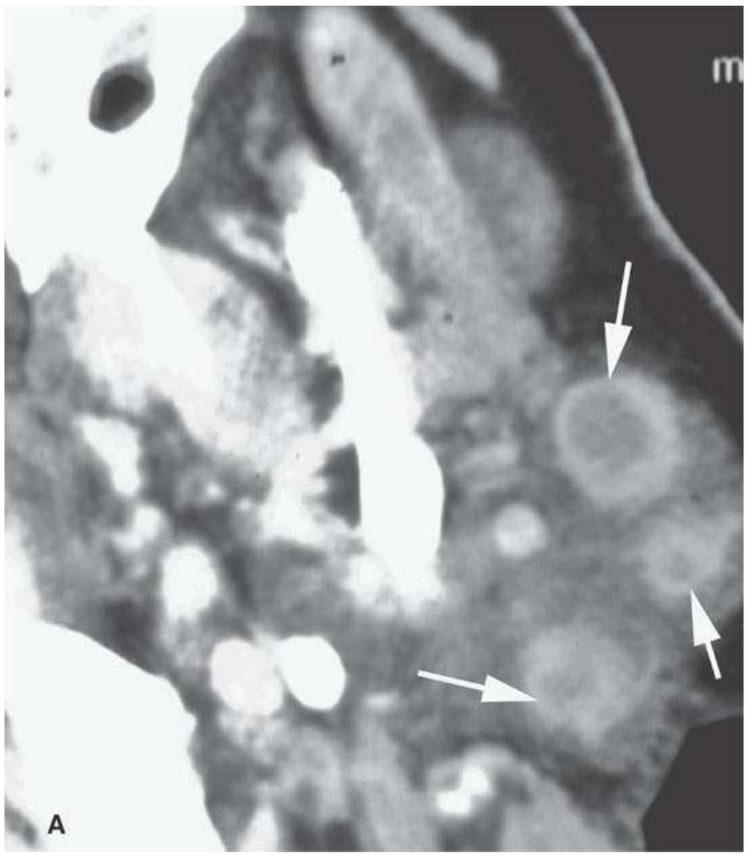
A

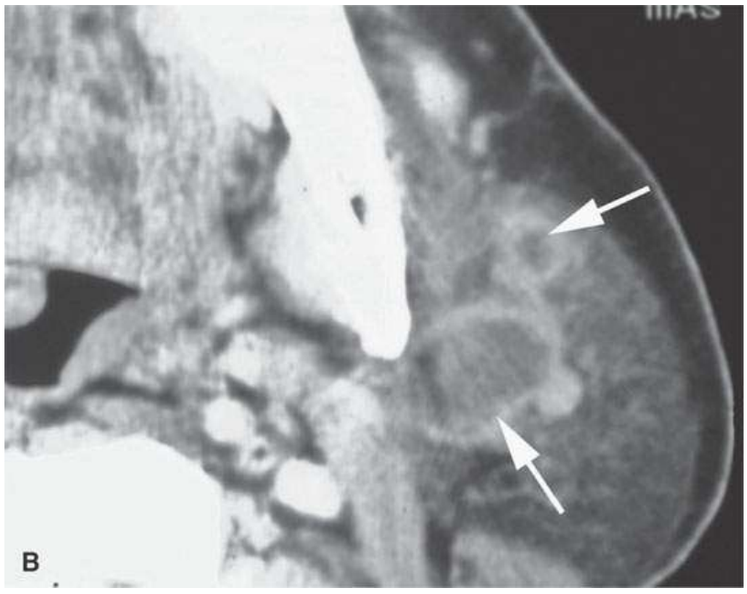
B

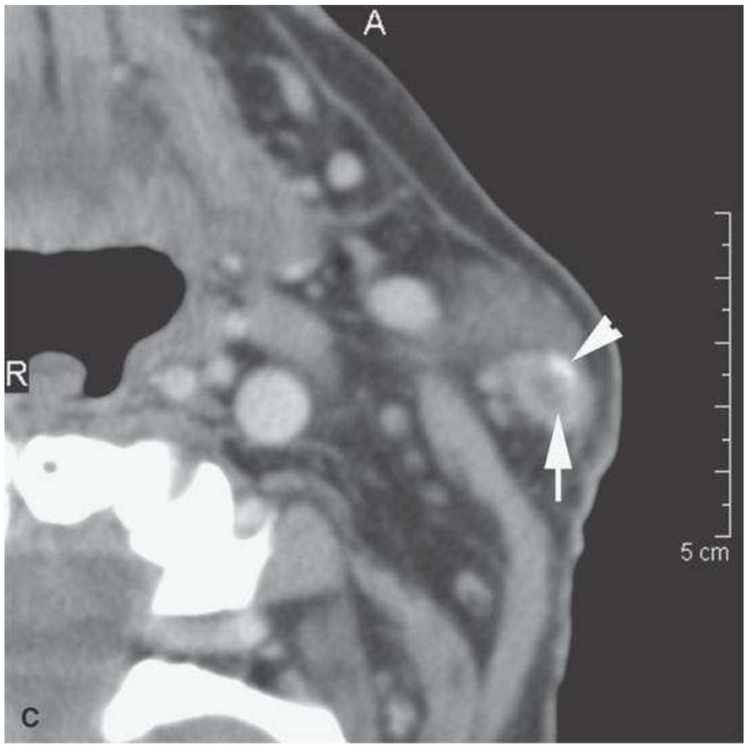
A
R
5 cm
C

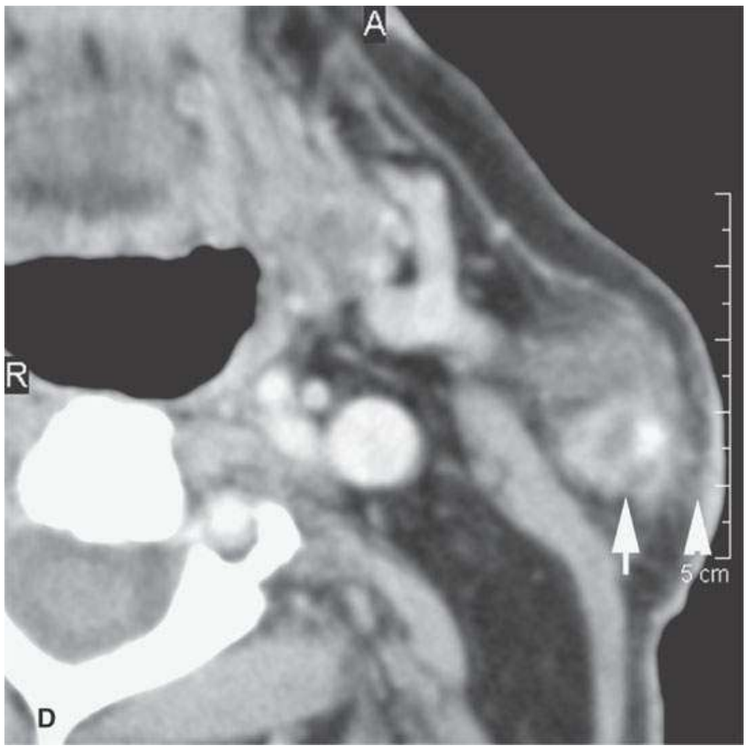
A
R
5 cm
D

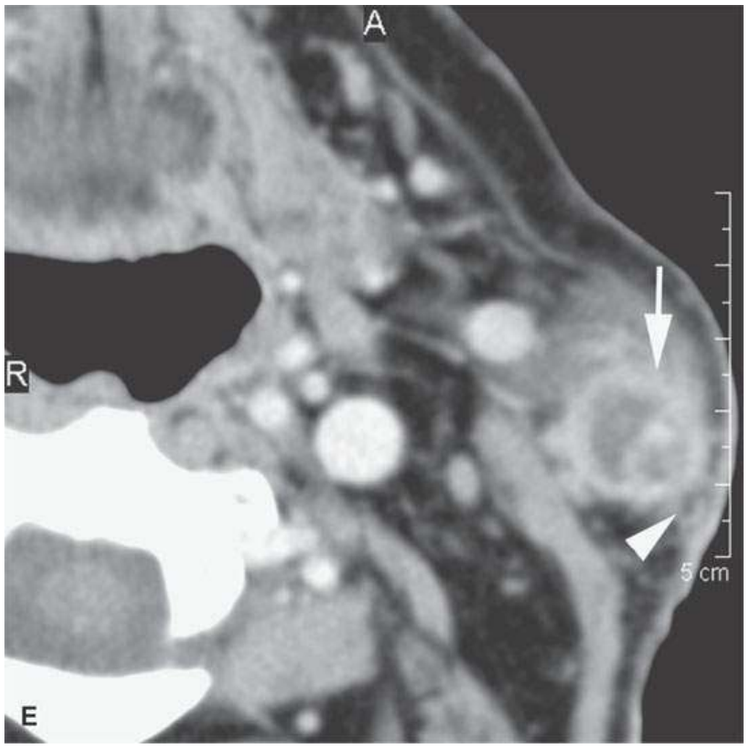
A
R
5 cm
E

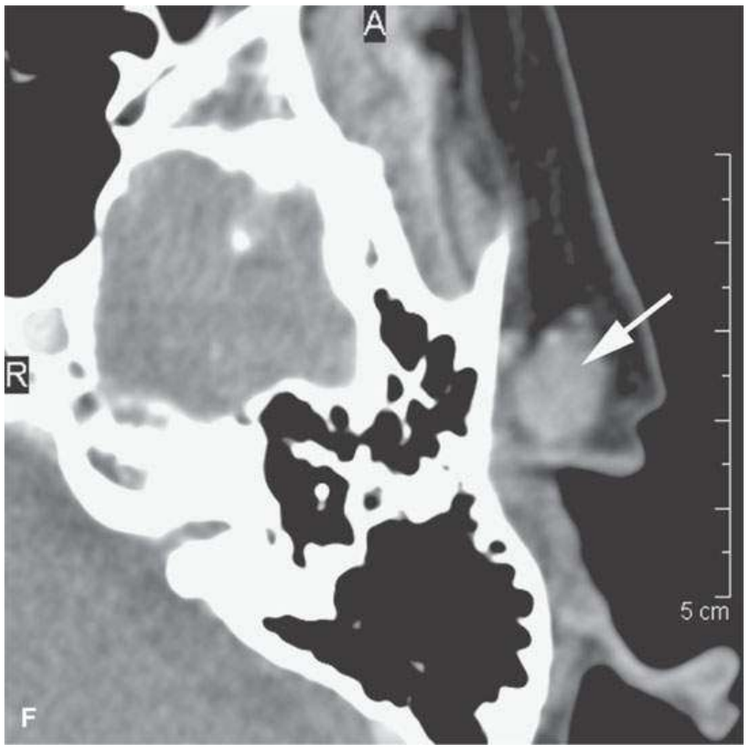
A
R
5 cm
F

FIGURE 24.12. Contrast-enhanced computed tomography of a patient with squamous cell carcinoma of the temple region in a typical distribution of intra- and periparotid nodes *(arrows)* within the gland **(A, B)**, at the tail of the gland **(C, D)**, and in the pretragal region **(E).** Most of the nodes show focal metastatic defects *(arrows)* and evidence of extranodal spread *(arrowheads)*.

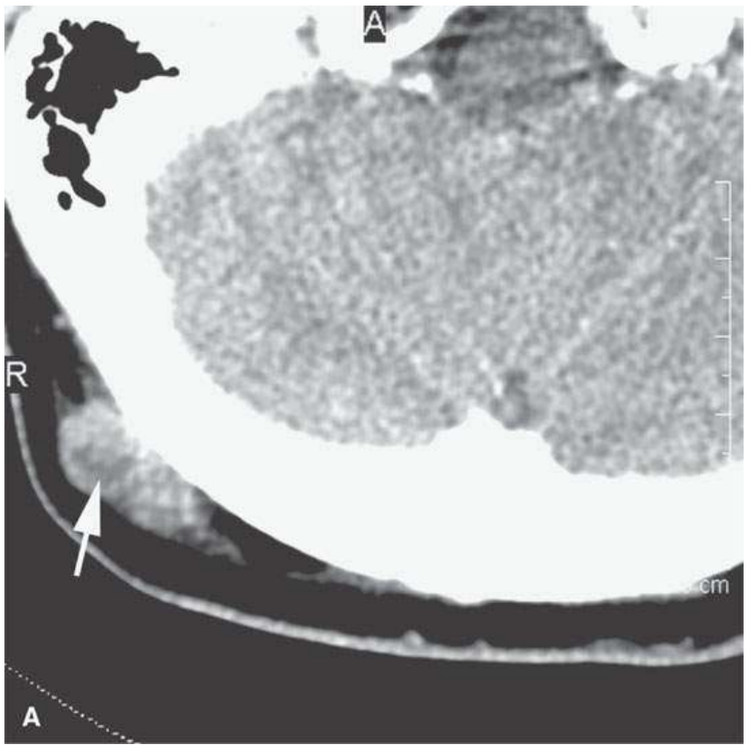

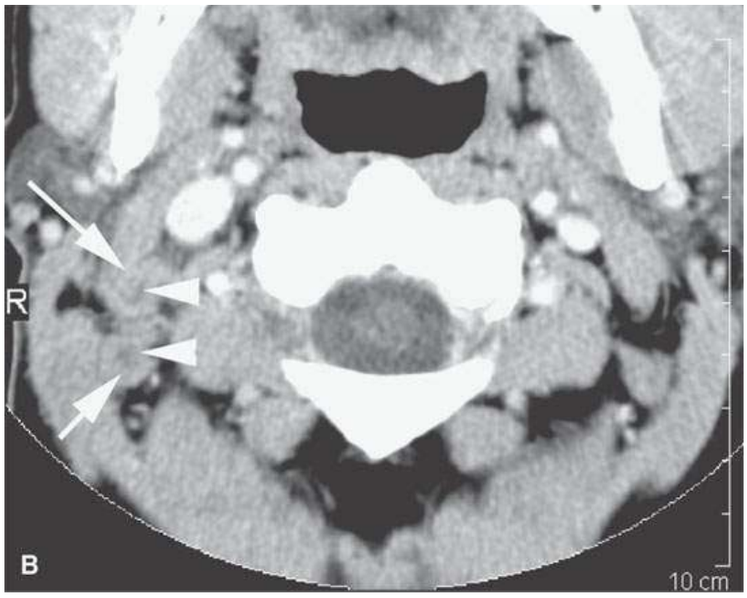

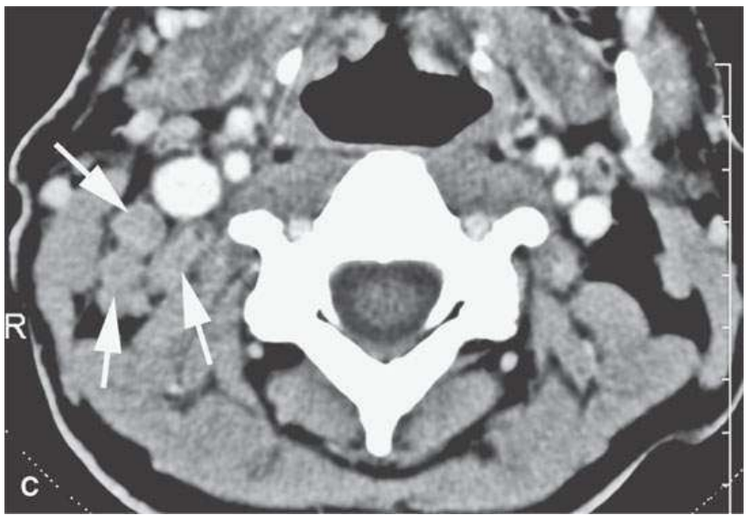

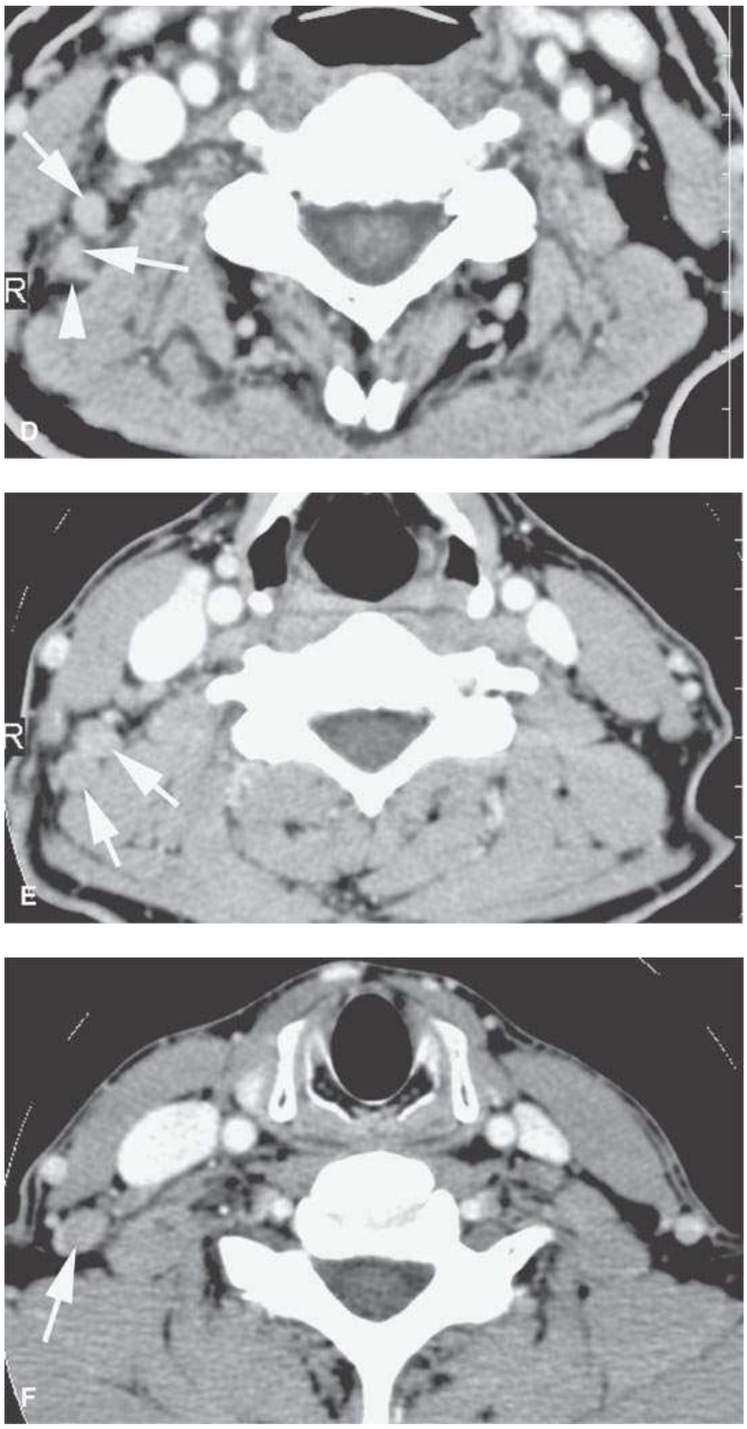

FIGURE 24.13. Contrast-enhanced computed tomography of a patient with squamous cell carcinoma of the posterior scalp region in a typical distribution for such a skin cancer**. A:** Posterior neck node *(arrow)* with an obvious focus of metastatic disease**. B–F:** Multiple abnormal nodes *(arrows)* clustering and some with focal *(arrowheads)* defects predominantly in the posterior triangle, including levels 2B, 3, 5A, and 5B**.**When this pattern is seen, a skin primary should be considered the most likely etiology**.** When a known primary is studied, the posterior neck group must be fully evaluated**.**

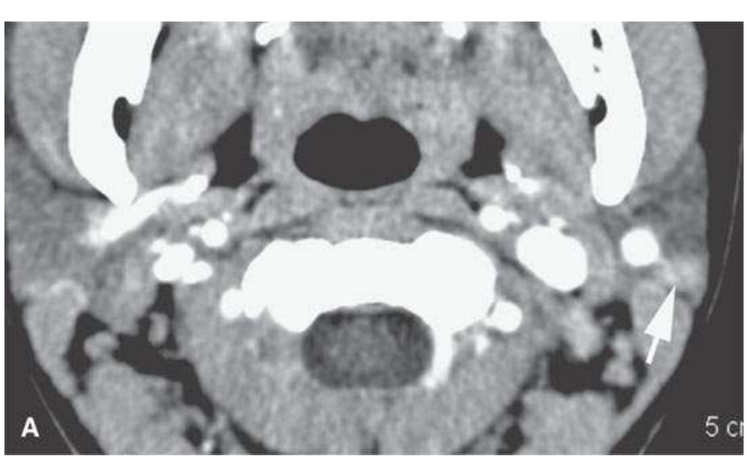

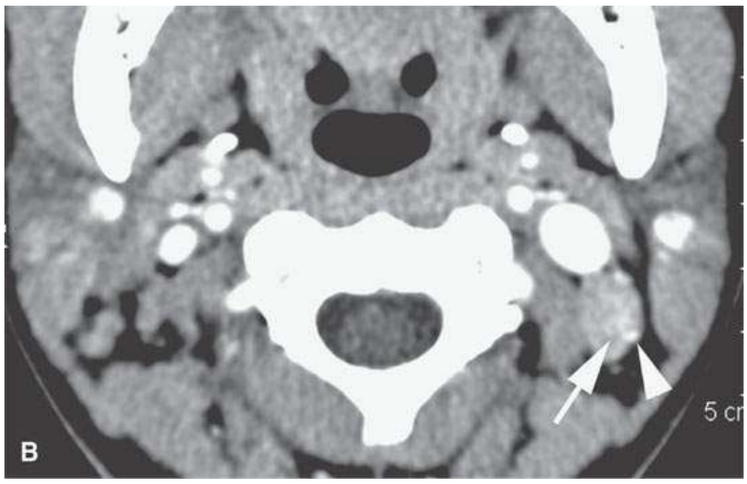

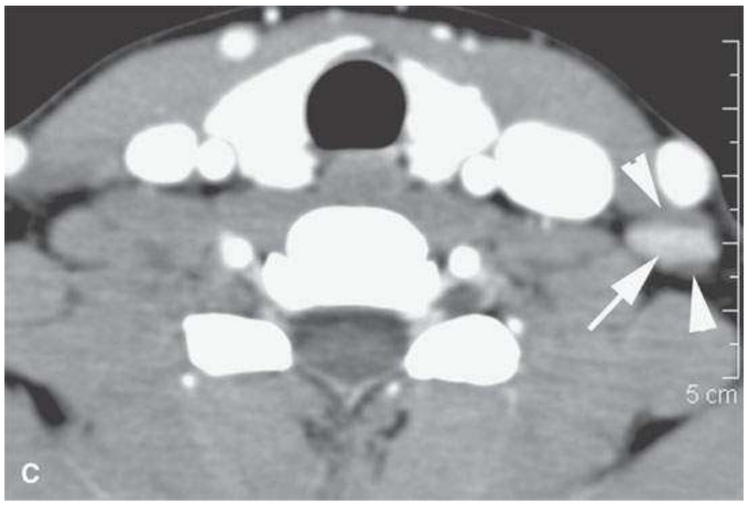

FIGURE 24.14. Contrast-enhanced computed tomography of a patient with squamous cell carcinoma of the periauricular region in a typical distribution for such a skin cancer. **A**: The small node at the parotid tail is suspicious based on small zones of focal enhancement *(arrow)*. **B**: Level 2B node is positive based on the focal areas of abnormal enhancement and/or keratin debris collections and calcification. **C**: Level 5B node is positive based on focal central enhancing focus arrow.

PATHOLOGY

Basal cell carcinoma accounts for about two thirds of skin cancer and squamous cell carcinoma (SCCA) for almost one third.[3] Melanoma is less common but far more morbid with respect to treatment of advanced disease and deadly.[4] Merkel cell carcinoma is a rare neuroendocrine malignancy arising in the skin.[5] SCCA, melanoma, and Merkel cell carcinoma all carry a risk of perineural invasion at presentation (Fig. 24.5). Perineural spread in basal cell carcinoma usually is seen following one or more recurrences at the primary site. The rate of perineural spread is increased in all histologic types if tumor is recurrent.

Most basal and squamous cell cancers remain superficial for a long period of time. Eventually, they will penetrate the dermis to invade subcutaneous and other underlying structures (Fig. 24.11). Occasionally, these cancers will grow predominantly beneath the skin—a pattern that is more common in recurrent disease and can lead to gross underestimation of tumor extent at physical examination (Fig. 24.11). Advanced basal cell and squamous cell cancers will invade cartilage and bone and show perineural spread, and SCCA will commonly spread via the lymphatics (Figs. 24.1–24.14). Lymphatic spread in basal cell carcinoma in particular has a very low rate of regional nodal involvement even in recurrent disease. Melanoma and Merkel cell cancer show the same general behavior as SCCA but on a relatively accelerated time line except for less well differentiated SCCA (Figs. 24.15 and 24.16).

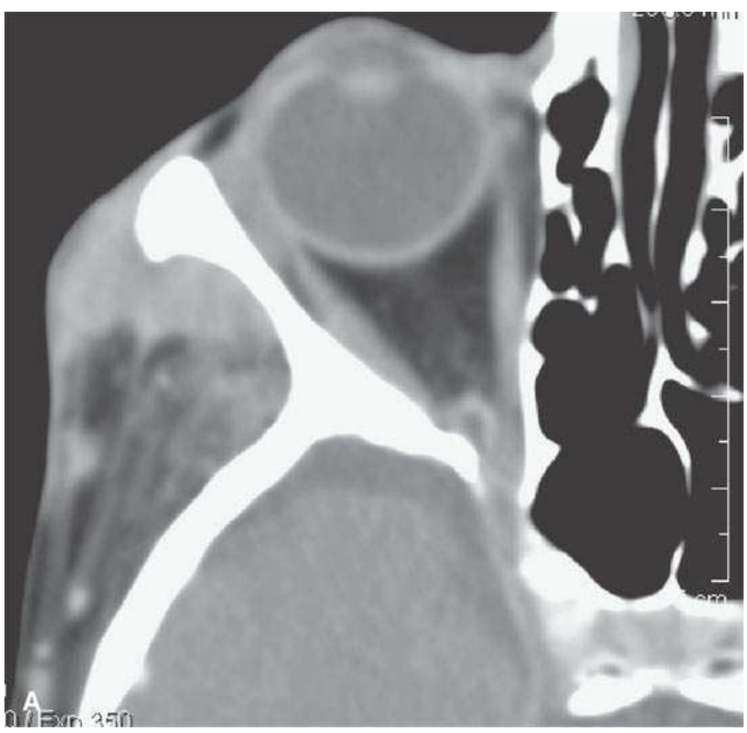

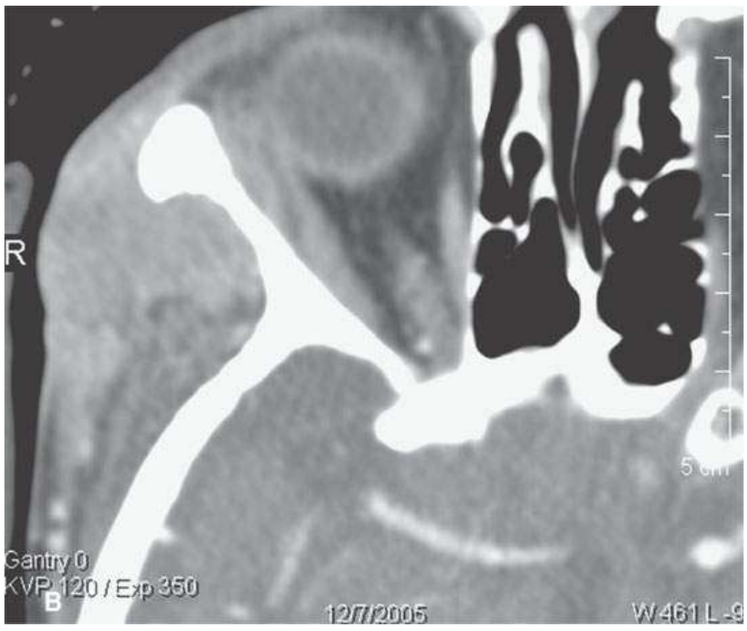

FIGURE 24.15. Contrast-enhanced computed tomography of a patient with a rapidly progressive malignant melanoma**.** The studies in **(A)** and **(B)** are only 2 months apart**.**

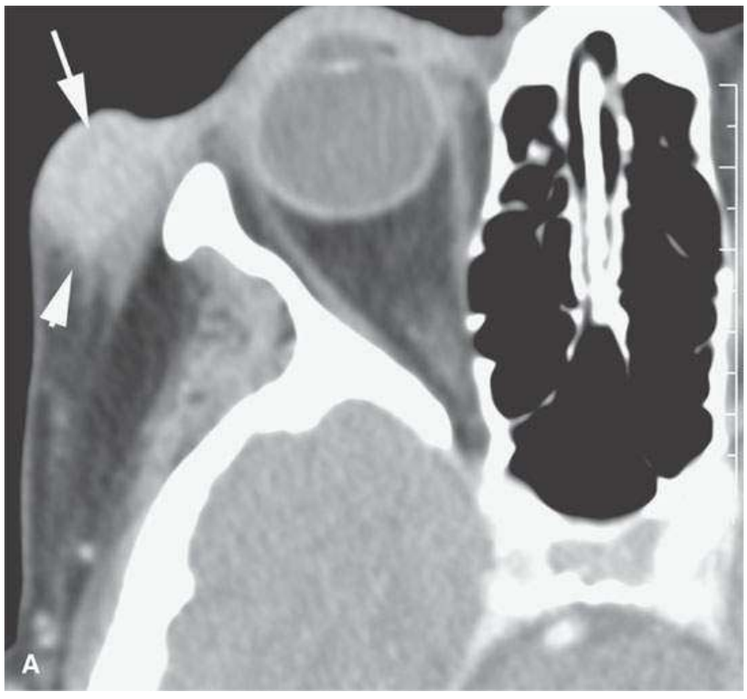

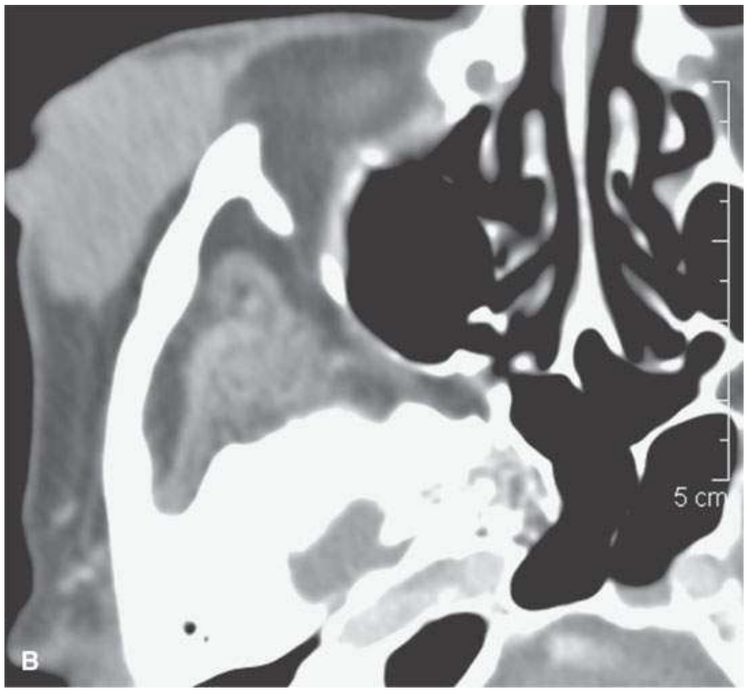

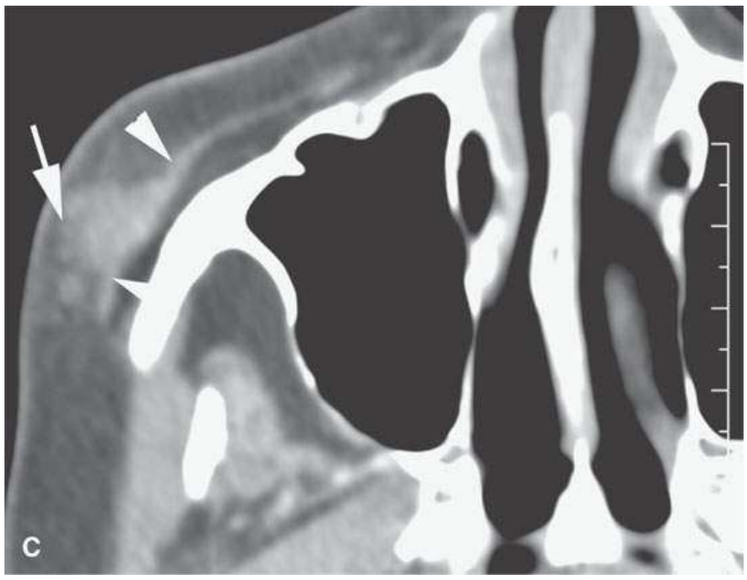

FIGURE 24.16. Contrast-enhanced computed tomography of a patient with a Merkel cell carcinoma which is typically a rapidly spearing tumor. **A, B:** The mass *(arrow)* has a potentially aggressive deep margin *(arrowhead in **A**)*. **C:** The tumor *(arrow)* tends to remain in the subcutaneous soft tissues and spreads along the superficial aspect of the superficial musculoaponeurotic system, which is thickened *(arrowheads)*.

Distant metastasis is unusual in SCCA and rare in basal cell cancer. Basal-squamous or so-called metatypical basal cell carcinoma behaves more like SCCA. Melanoma and Merkel cell cancers have a much greater chance of dissemination with distant metastatic spread (Figs. 24.17 and 24.18).

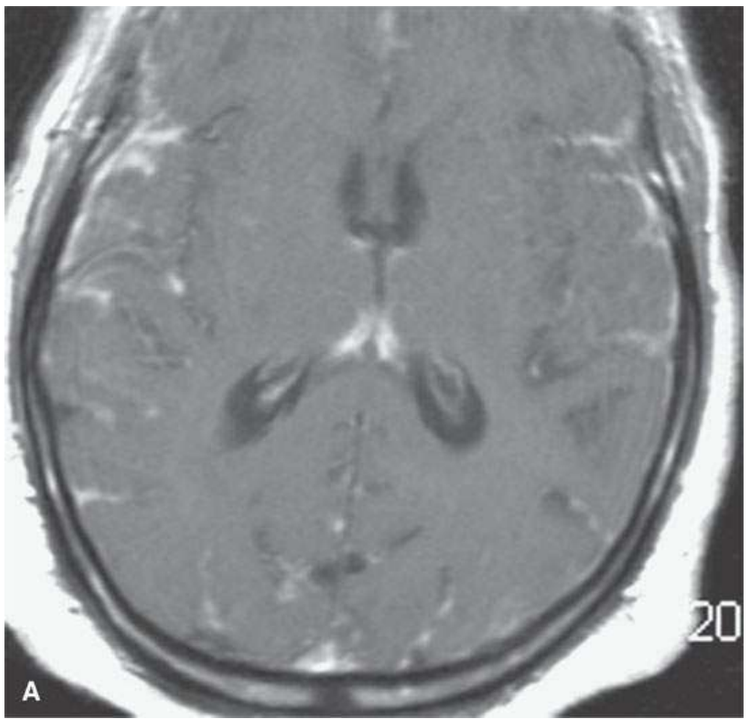

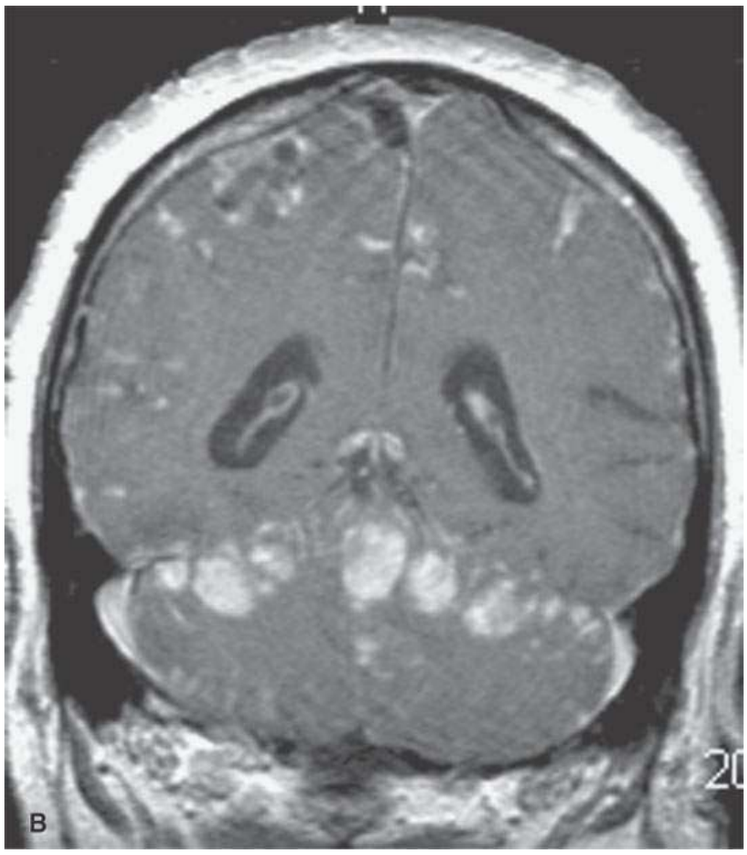

FIGURE 24.17. Contrast-enhanced computed tomography showing diffuse leptomeningeal dissemination of Merkel cell carcinoma.

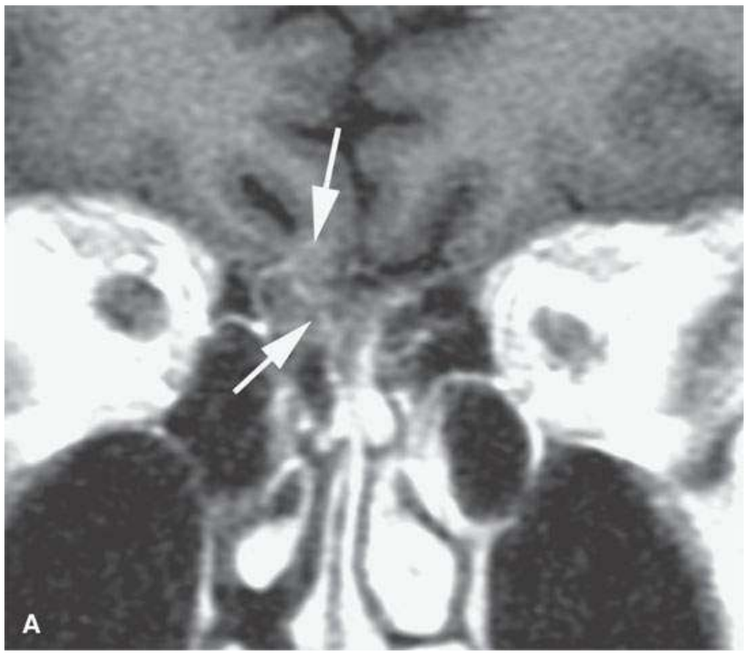

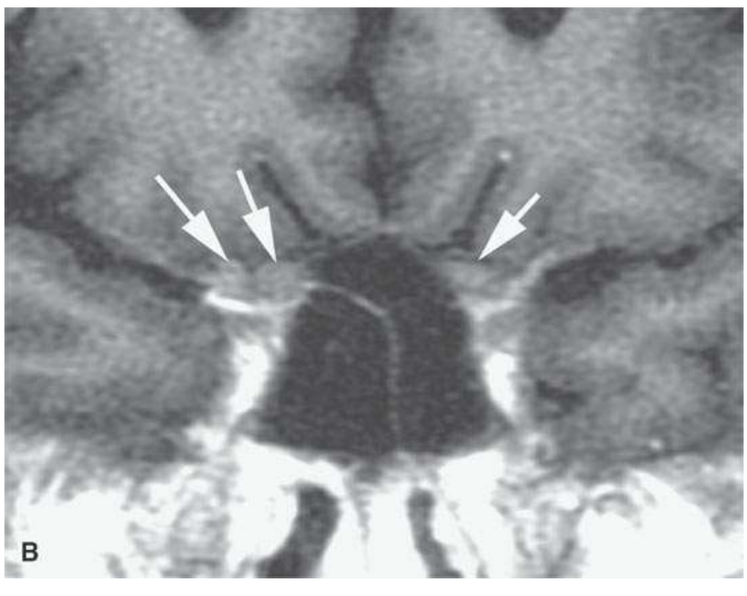

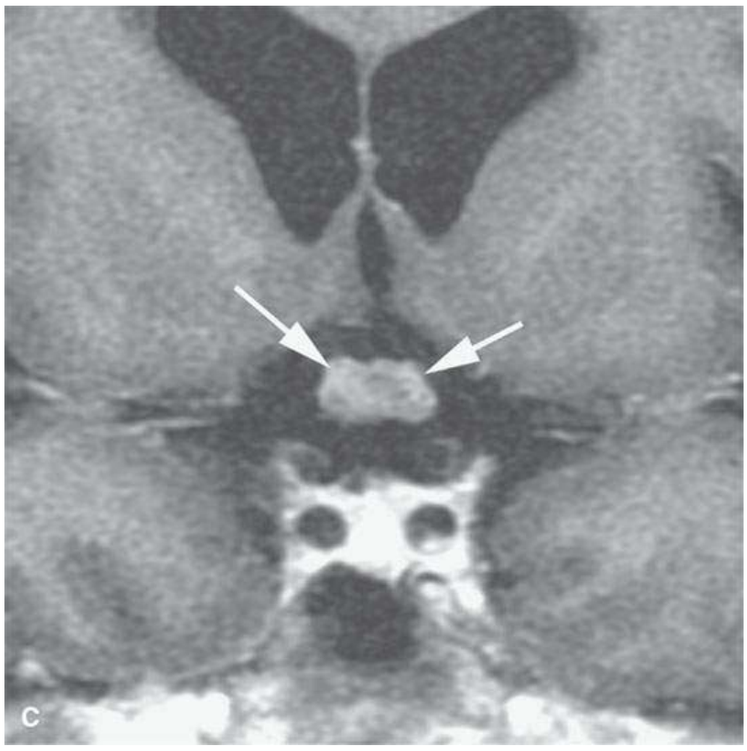
C

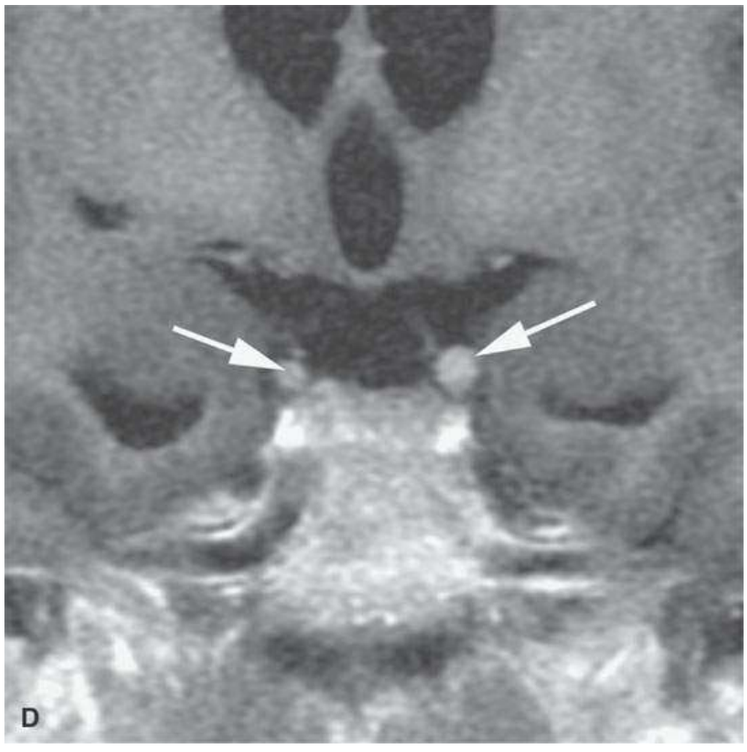
D

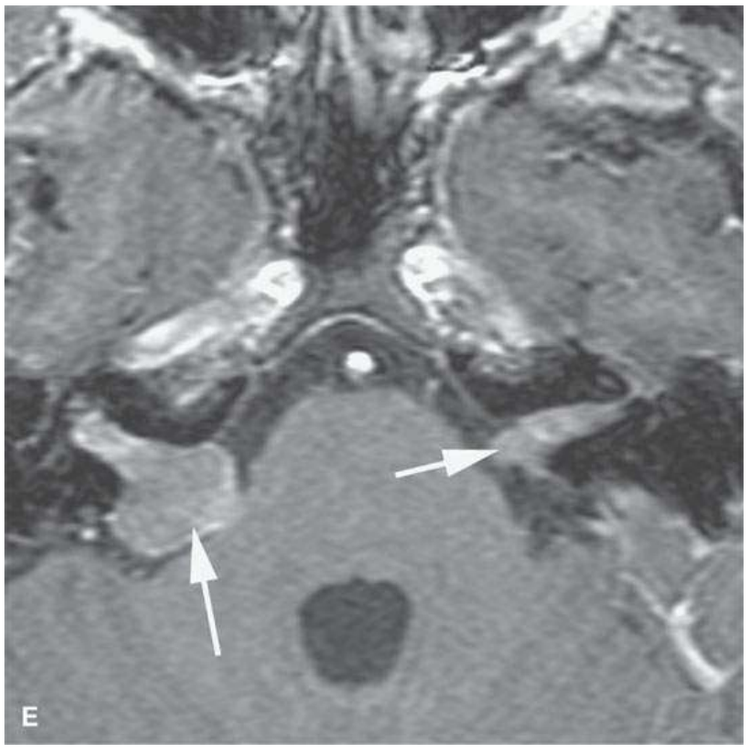
E

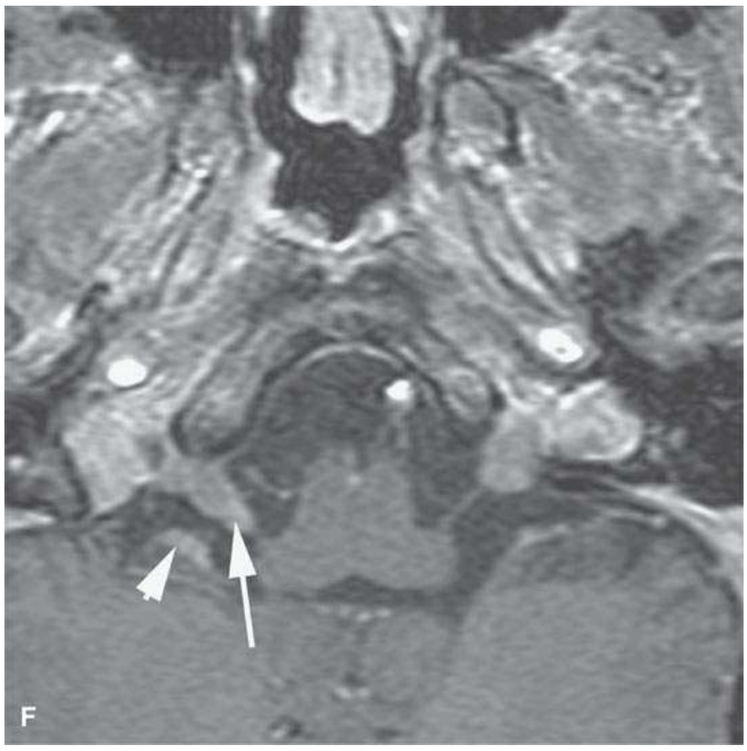
F

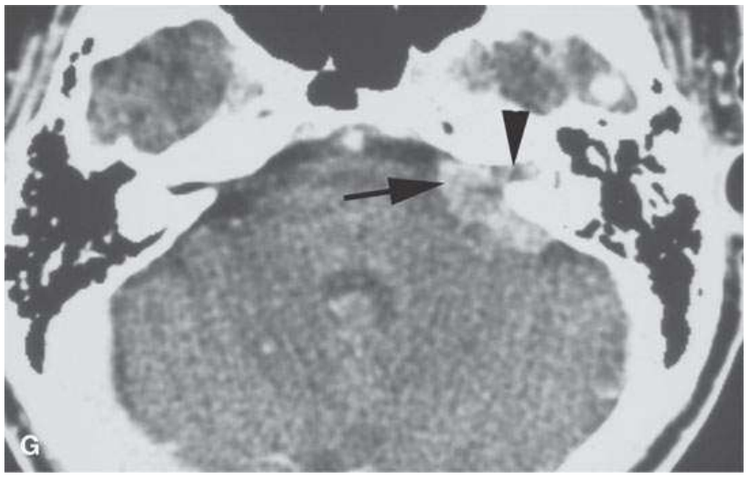
G

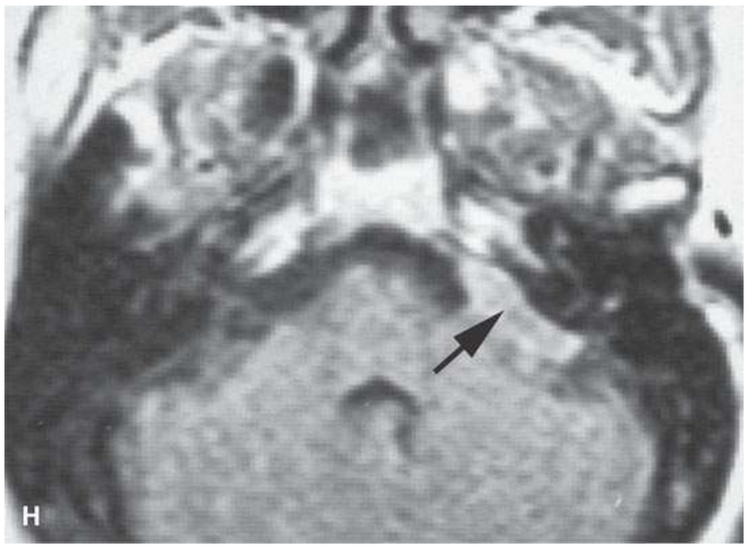
H

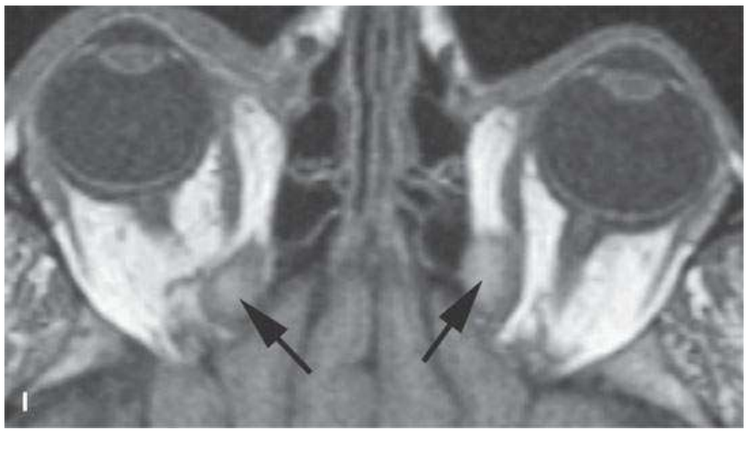
I

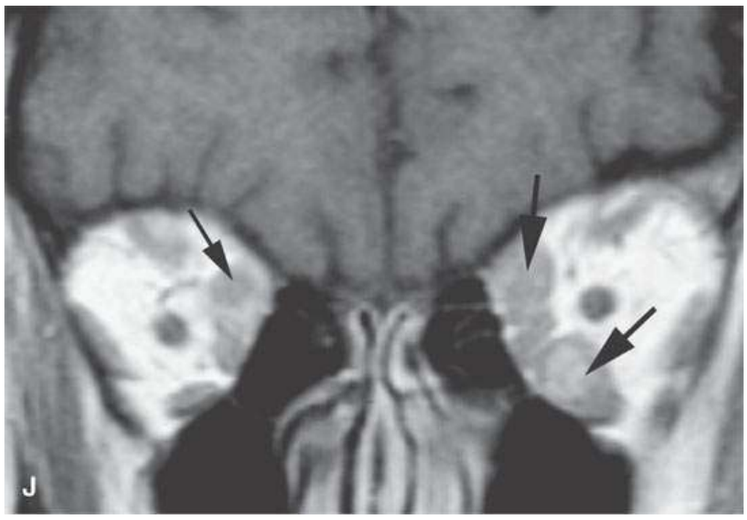

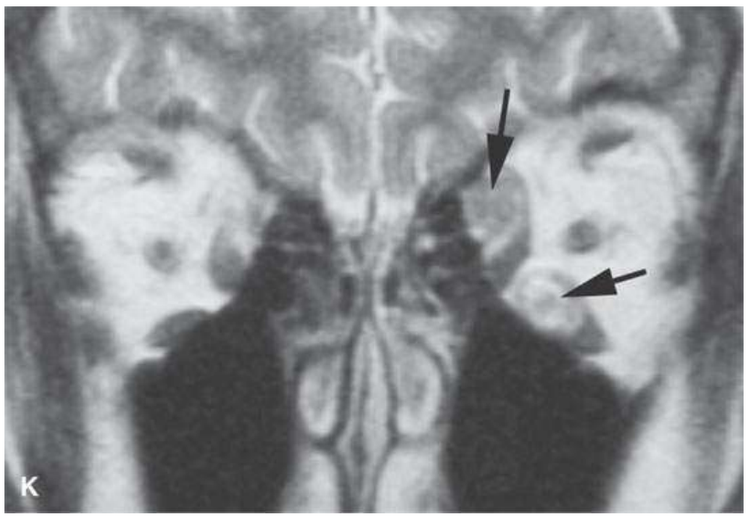

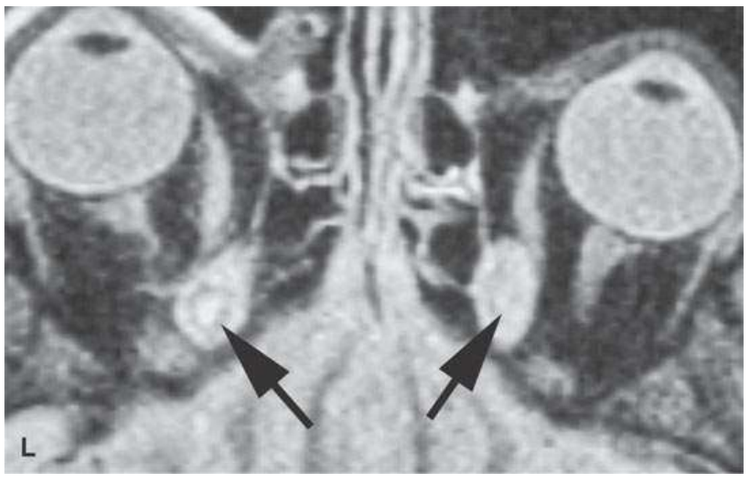

FIGURE 24.18. Three patients with disseminated extracranial and intracranial melanoma from primaries on the face**.**TI-weighted (T1W) contrast-enhanced images of a patient with a combination of leptomeningeal and neurotropic spread**.** The *arrows* in all images show tumor "caked" around various cranial nerves and including the olfactory tract **(A)** and optic nerve and chiasm and third cranial nerves and both 7th and 8th nerve complexes **(B, C,D,–E). F:** There is spread along the cranial nerves in the jugular fossa and a focus of pia arachnoid spread *(arrowheads)*; the latter not along a cranial nerve*(arrowheads)***. G:** Contrast-enhanced computed tomography of a dural-based metastasis *(arrows)* in the cerebellopontine angle that is of higher signal intensity than the brain on both the CT and the comparison non–contrast-enhanced T1W image in **(H).**Magnetic resonance imaging of a patient with ocular motility disturbance due to multiple melanoma metastases *(arrows)* to the extraocular muscles**. I:** Non–contrast-enhanced T1W image showing the inherently increased signal intensity of the melanoma metastases to the muscle, possibly reflecting a melanin effect**. J:** Contrast-enhanced T1W image**. K:** T2-weighted image**. L:** Short T1 inversion recovery (STIR) image**.**

Cancers arising from the sweat and sebaceous glands tend to occur around the eyelids, face, and scalp**.** They may have a significant volume beneath the skin surface (Fig. 24.19)**.** These tend to behave like SCCA**.**

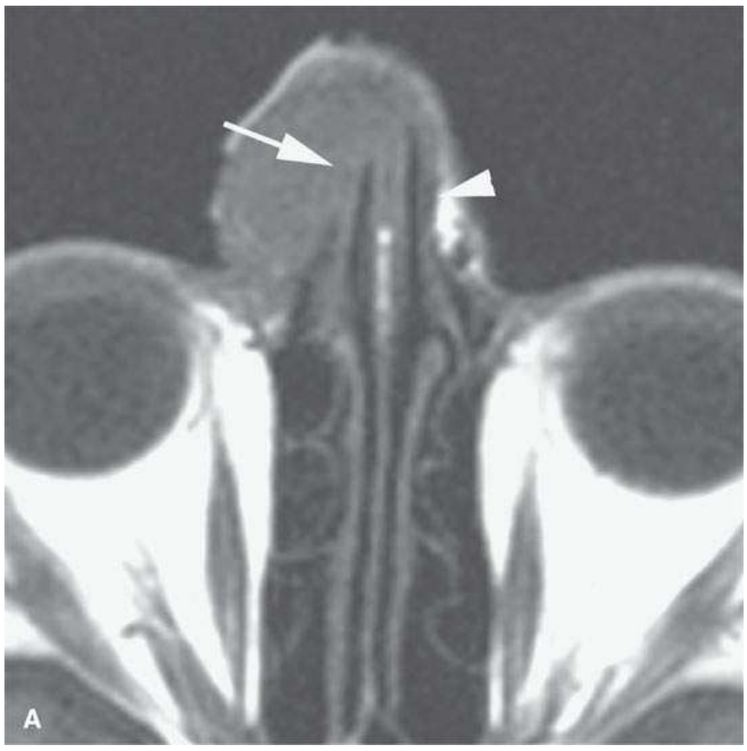
A

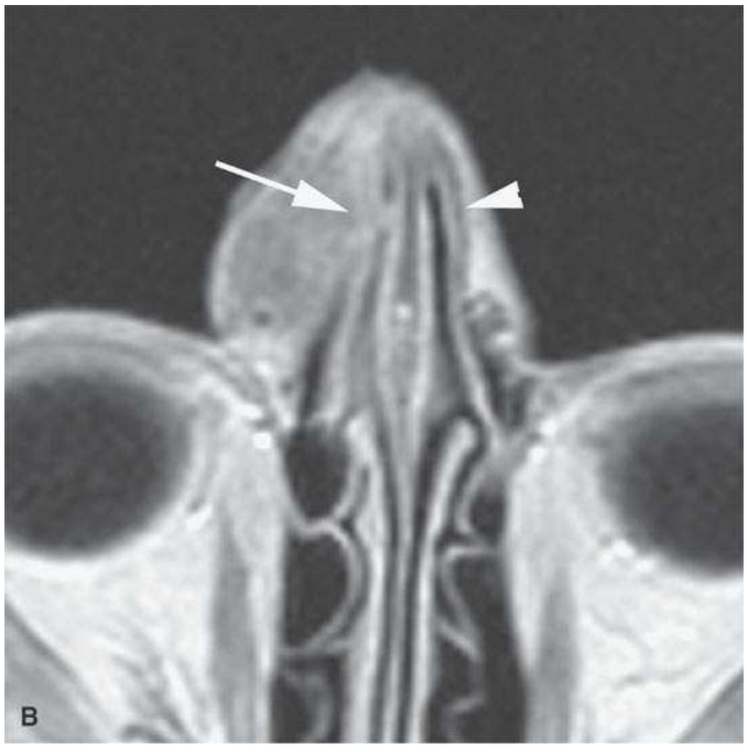
B

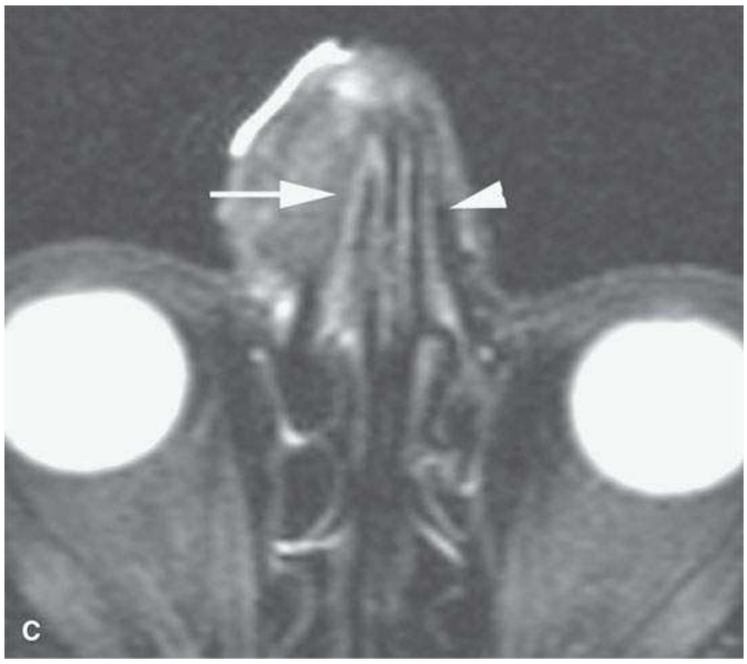
C

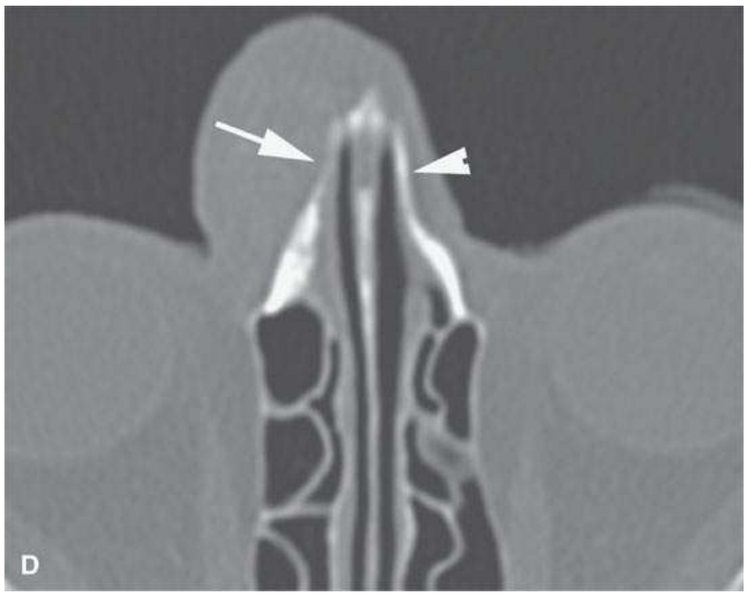
D

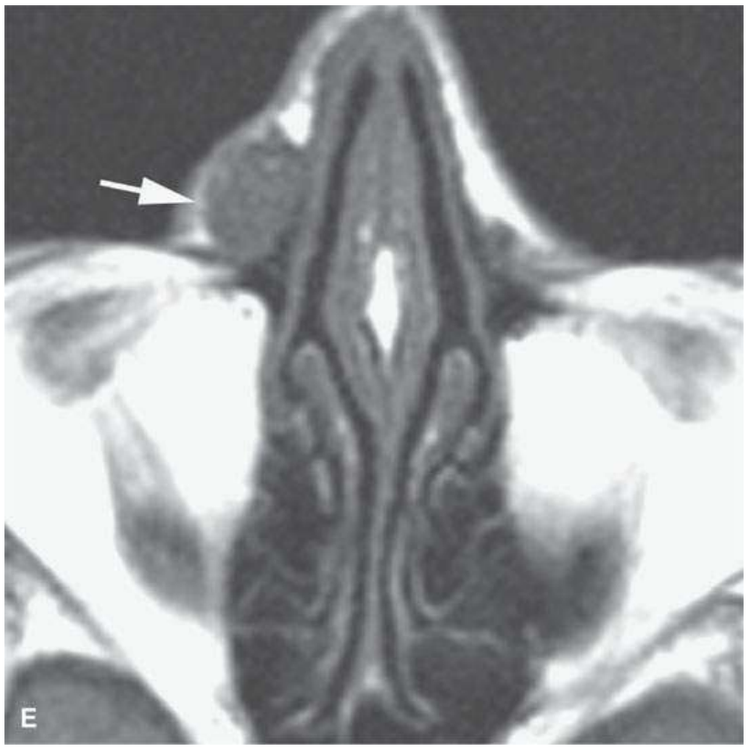
E

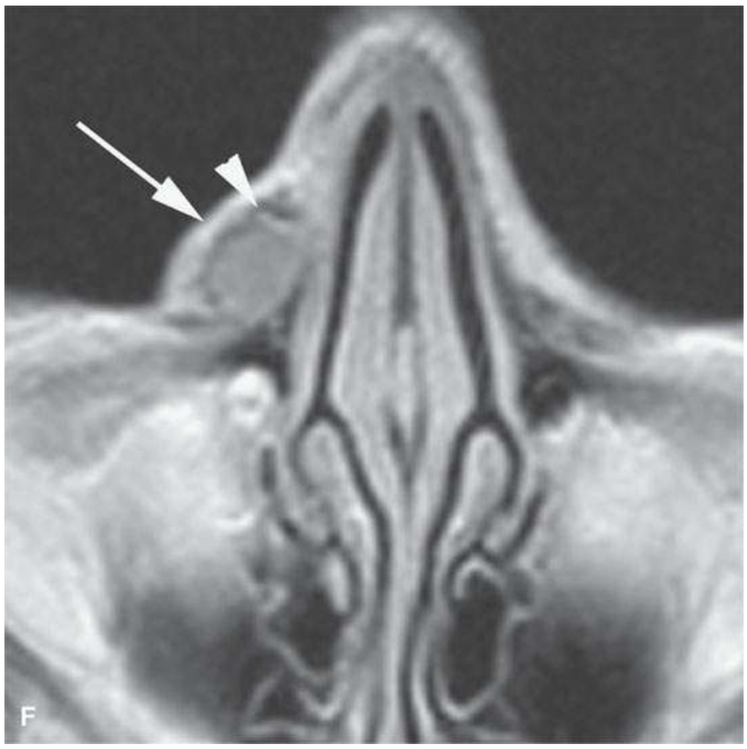
F

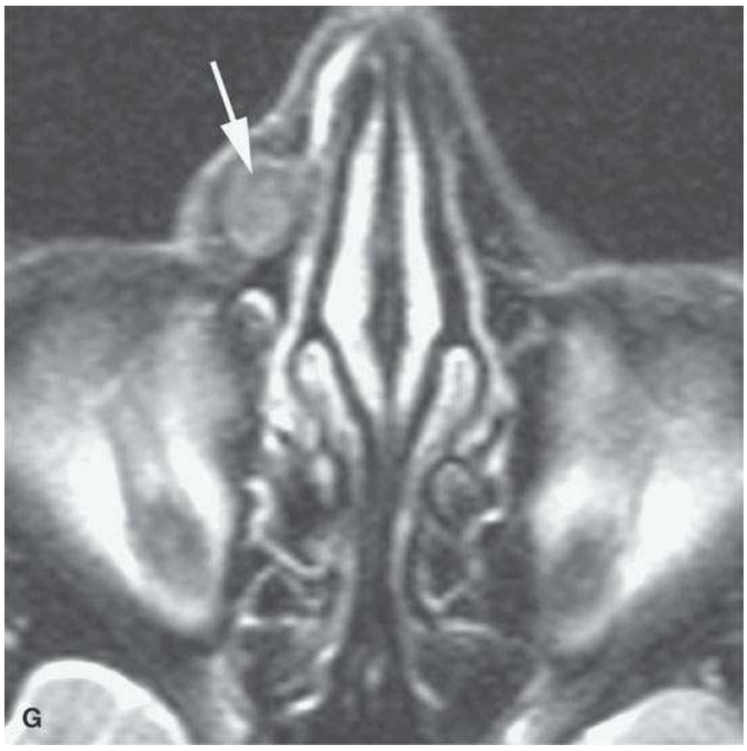
G

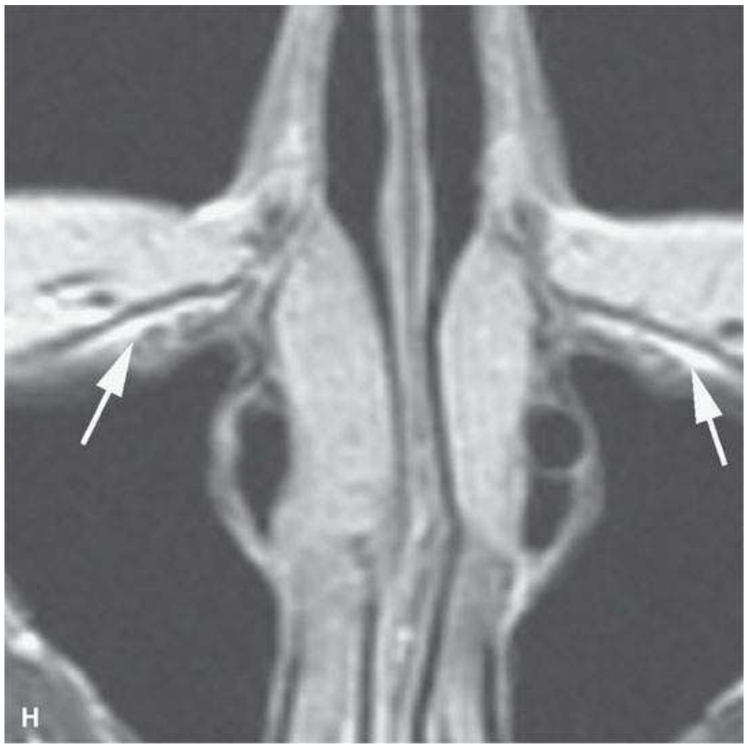
H

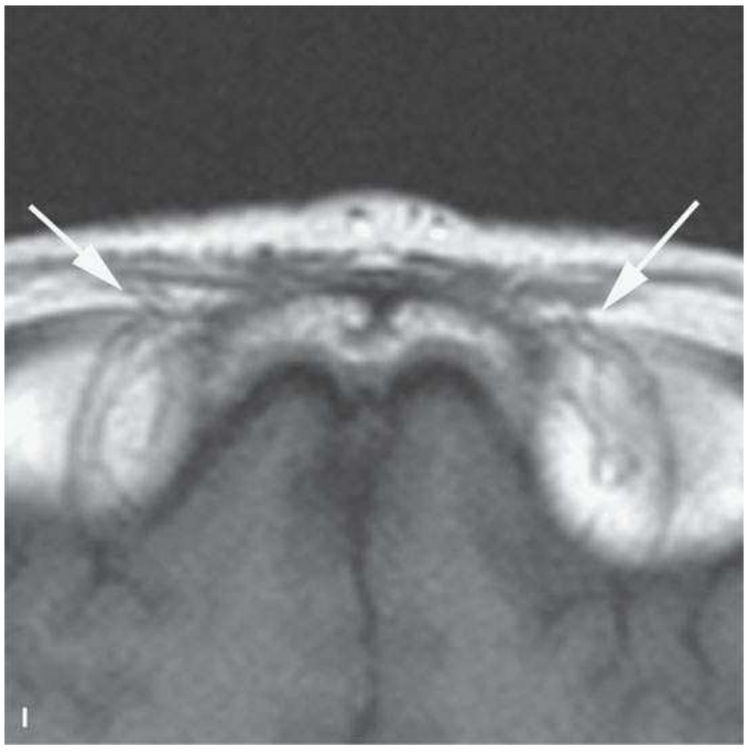
I

FIGURE 24.19. Magnetic resonance imaging (MRI) of a patient with sebaceous cell carcinoma of the nose invading the nasal cartilages *(arrows)* as compared to the opposite normal side *(arrowhead)* seen in **(A)** through **(C)**. Bone involvement is uncertain but confirmed by computed tomography (*arrow* in **D**) compared to the normal opposite side *(arrowhead)*. **E–G**: MRI shows continued spread beneath the superficial musculoaponeurotic system *(arrows)* and sparing the subcutaneous fat, *((arrowheads)* an extension that was difficult to appreciate clinically. **H, I**: MRI that excludes gross perineural spread along the infraorbital and supraorbital nerves, respectively *(arrows showing normal neurovascular bundles beneath SMAS*).

A significant proportion of Merkel cell carcinomas arise in the head and neck region.5 The lesion is usually <2 cm at presentation typically in a white man over 60 years old. The tumor tends to spread superficially very rapidly and metastasize early to regional parotid, level 1, and level 2 nodes. Distant metastases also occur early in the natural history of the disease (Figs. 24.16 and 24.17).

In skin cancer, the risk of lymphatic spread increases with the size of the lesion, depth of penetration, and histologic grade. Recurrent disease is also more likely to involve nodes, and that involvement may be the actual presentation of recurrence either from an inconspicuous subdermal primary failure or just a regional failure (Fig. 24.12). If the parotid nodes are positive, the ipsilateral neck is likely to be positive as well. Parotid nodes are most likely to be involved in the preauricular region or tail of the gland (Fig. 24.12).

Posterior scalp lesions metastasize to the occipital nodes. Parietal scalp cancers spread to the postauricular nodes (Fig. 24.13). Cancers of the frontal scalp, temple, and eyelids spread to the parotid area lymph nodes. Lesions of the nose and lips spread to the level 1 and parotid nodes (Fig. 24.10). All cancers of the face and more anterior scalp can spread to facial nodes near the site of primary origin (Figs. 24.10A and 24.11B).

These groups at primary risk drain to levels 2A and 2B and 5A and 5B. Level 5 nodes are more at risk, as the primary site origin moves more posteriorly (Figs. 24.13 and 24.14).

CLINICAL PRESENTATION

Skin cancer typically presents as a slow-growing mass of the skin or just beneath the skin surface. Pain only occurs in advanced lesions. Paresthesias and formications, a crawling feeling under the skin, indicate perineural spread. This can be an initial presenting complaint but is far more common as a symptom heralding recurrence. Diagnosis in this clinical setting may be delayed because the treating physicians do not associate the history of skin cancer with signs of trigeminal or facial nerve dysfunction. Also, the patient may forget to offer the history of a treated skin cancer or may not be aware that a treated skin lesion was cancer (Fig. 24.6). Patient neglect can lead to advanced lesions with bone and cartilage destruction, orbit invasion, and regional metastases and perineural spread at presentation.

Physical examination must include a careful assessment for regional lymph node metastases and findings suggesting fifth and seventh cranial nerve dysfunction. Lymphadenopathy may be noted at initial presentation within months after initial treatment. However, nodal metastases not infrequently will show up for ≥5 years after the primary cancer is treated. Parotid region adenopathy, when so delayed, may be incorrectly attributed to primary SCCA of the parotid. Primary SCCA of the parotid is rare, and such an assumption can lead to a less than optimal treatment plan.

DIAGNOSTIC IMAGING

Computed tomography (CT) and/or magnetic resonance imaging (MRI) are used in a highly selected population of patients with skin cancer.6,7 CT is used for showing the soft tissue extent and bone and cartilage invasion as well as nodal metastases (Fig. 24.19). High-resolution MRI can refine the delineation of soft tissue extent when necessary and is the preferred study for assessing the full extent of perineural spread (Figs. 24.1–24.9). Fluorine-18 2-fluoro-2-deoxy-D-glucose positron emission tomography (FDG-PET) is particularly useful for detecting nodal metastases, even of small volume in melanoma and Merkel cell tumors. Sentinel node studies are commonly used as an adjunct to surgical treatment of the node, especially in melanoma. Ultrasound plays little role in evaluating the primary site. Some groups advocate its use for detecting and sampling parotid and cervical nodal metastases.6,8

Indications for Imaging

The dominant indications for with the use of CT and/or MRI in patients with skin cancer include the following.

Local Soft Tissue Extent

MRI shows invasion of deep muscles such as the temporalis and masseter and deep spaces of the face better than CT. Specific examples include extension medial to the temporomandibular joint and to and through the orbital septum (Figs. 24.20 and 24.21).

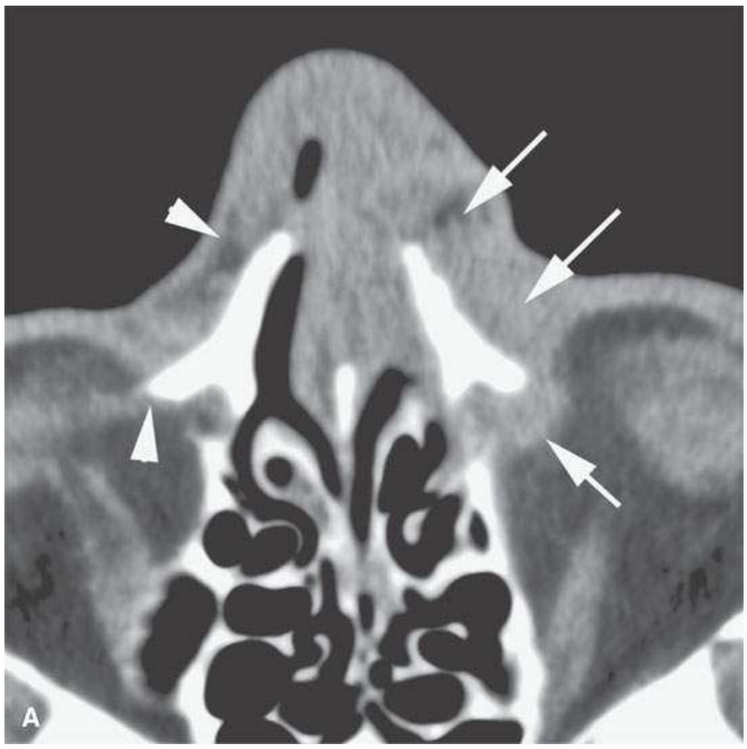

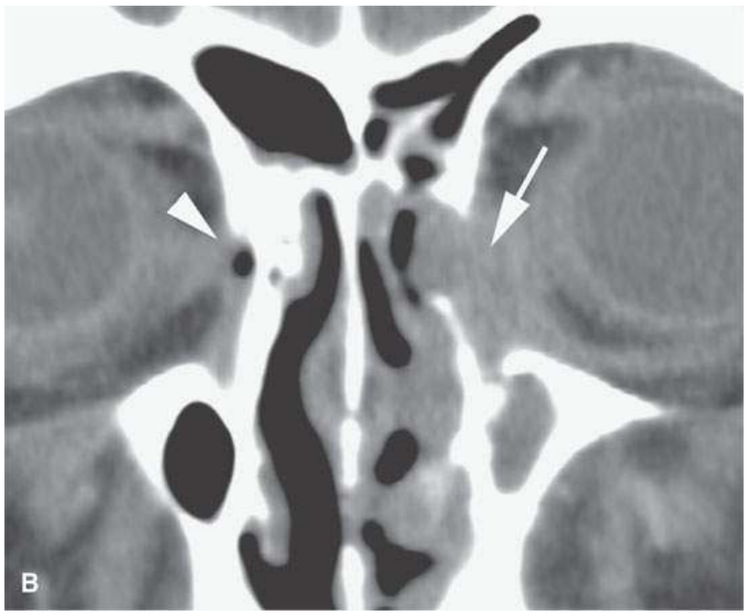
B

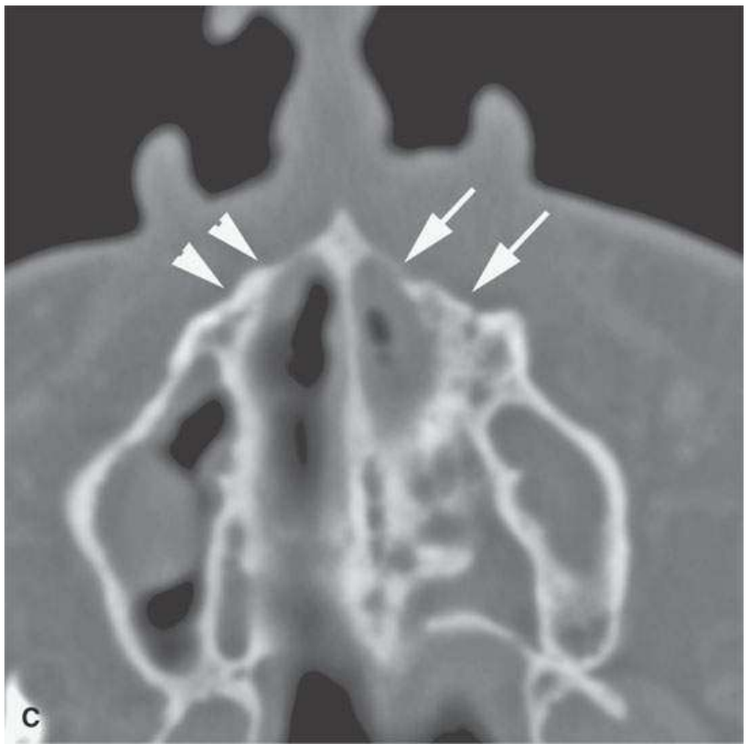
C

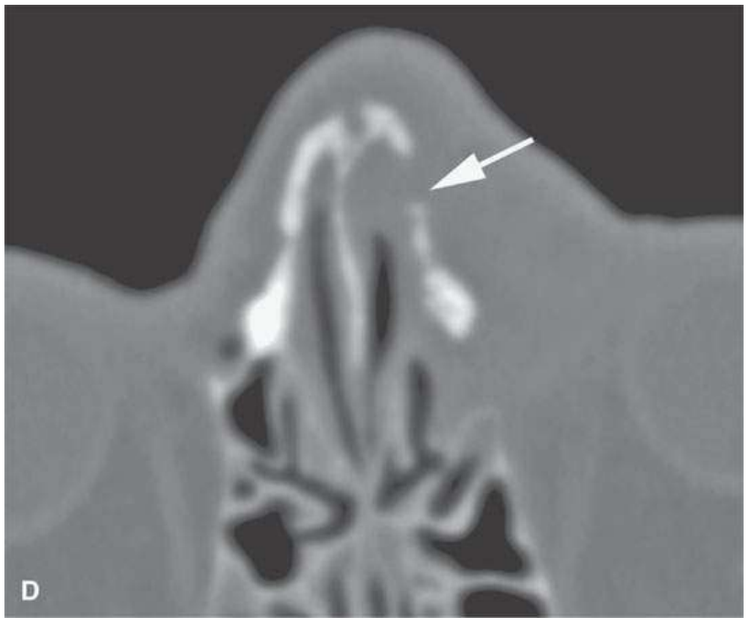
D

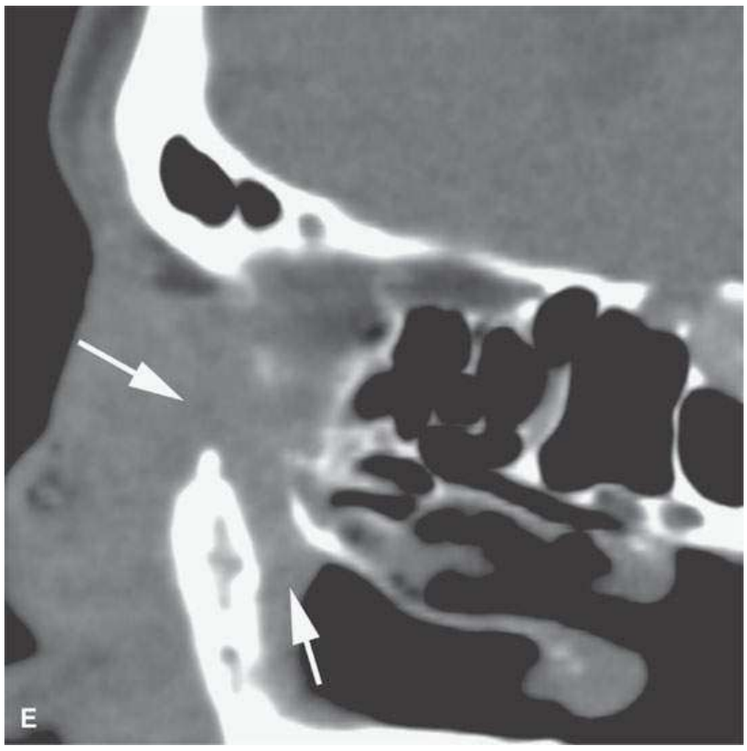
E

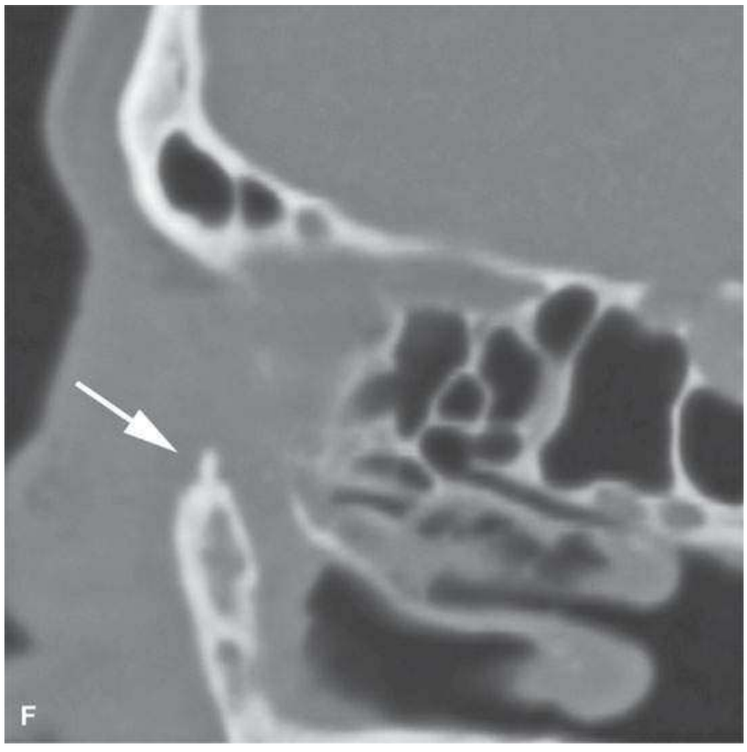
F

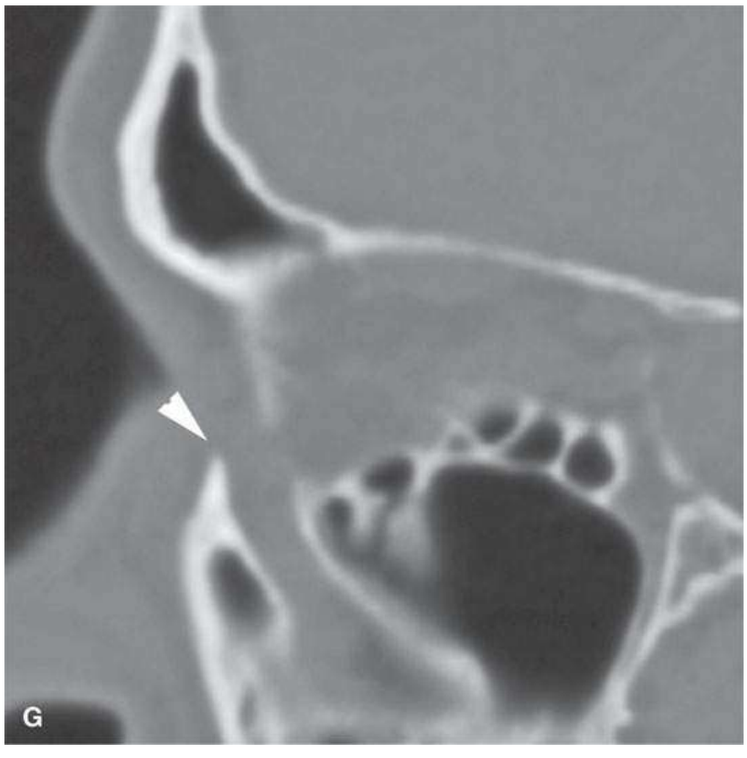
G

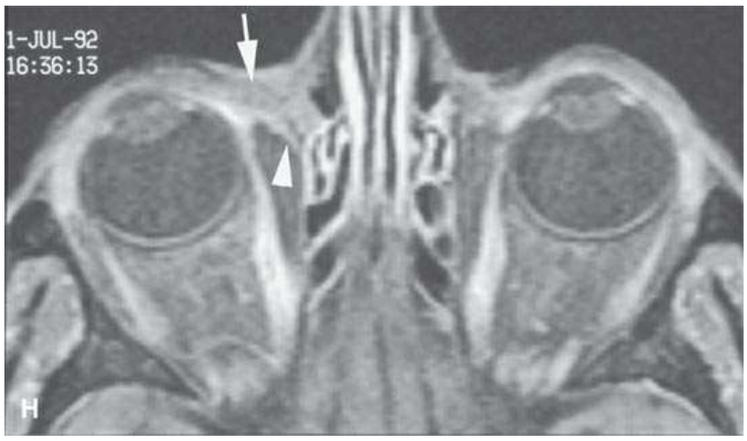

FIGURE 24.20. Patient with squamous cell carcinoma (SCCA) of the nasolabial fold felt clinically to be possibly deeply infiltrating based on palpable induration. **A, B:** Soft tissue involvement spreads to the attachment of the orbital septum on the posterior lacrimal crest *(arrows)* and into the nasolacrimal canal compared to the normal side *(arrowheads)*. **C:** Early bone erosion along the premaxilla *(arrows)* compared to normal side *(arrowheads)*. **D:** Nasal bone erosion *(arrow)*. **E:** Sagittal reformation showing spread into and likely involving the bone of the nasolacrimal canal *(arrows)*. **F:** Sagittal bone window of images in **(E)** show erosion and reactive changes of the bone of the canal *(arrows)* compared to the normal side **(G). H:** In another patient, contrast-enhanced T1-weighted images show a SCCA of the medial canthal region *(arrow)* spreading across the orbital septum *(arrowhead)*.

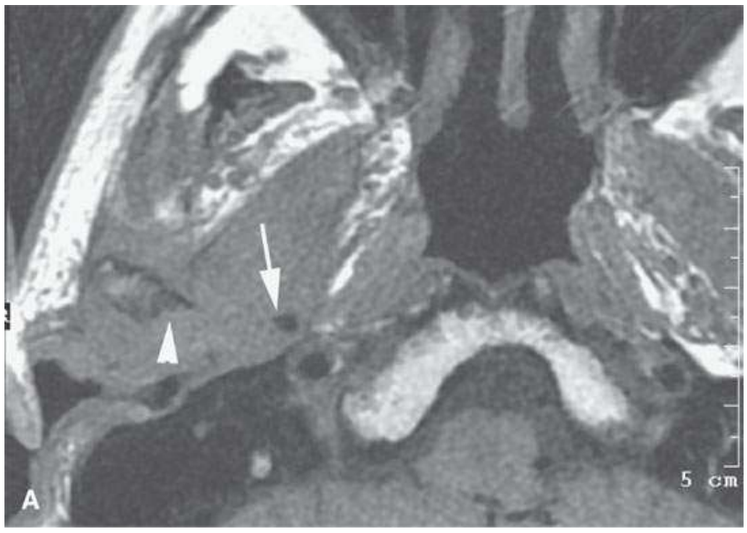

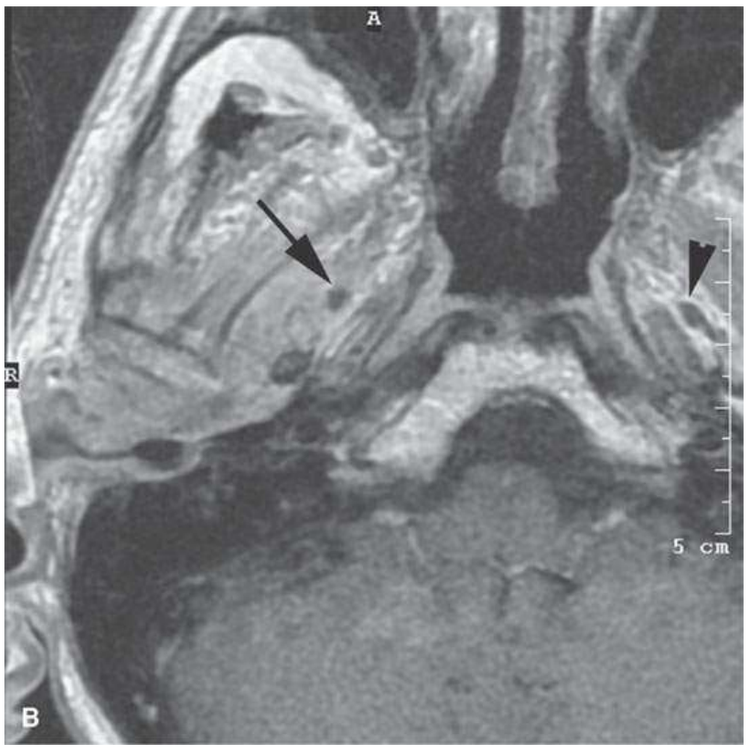

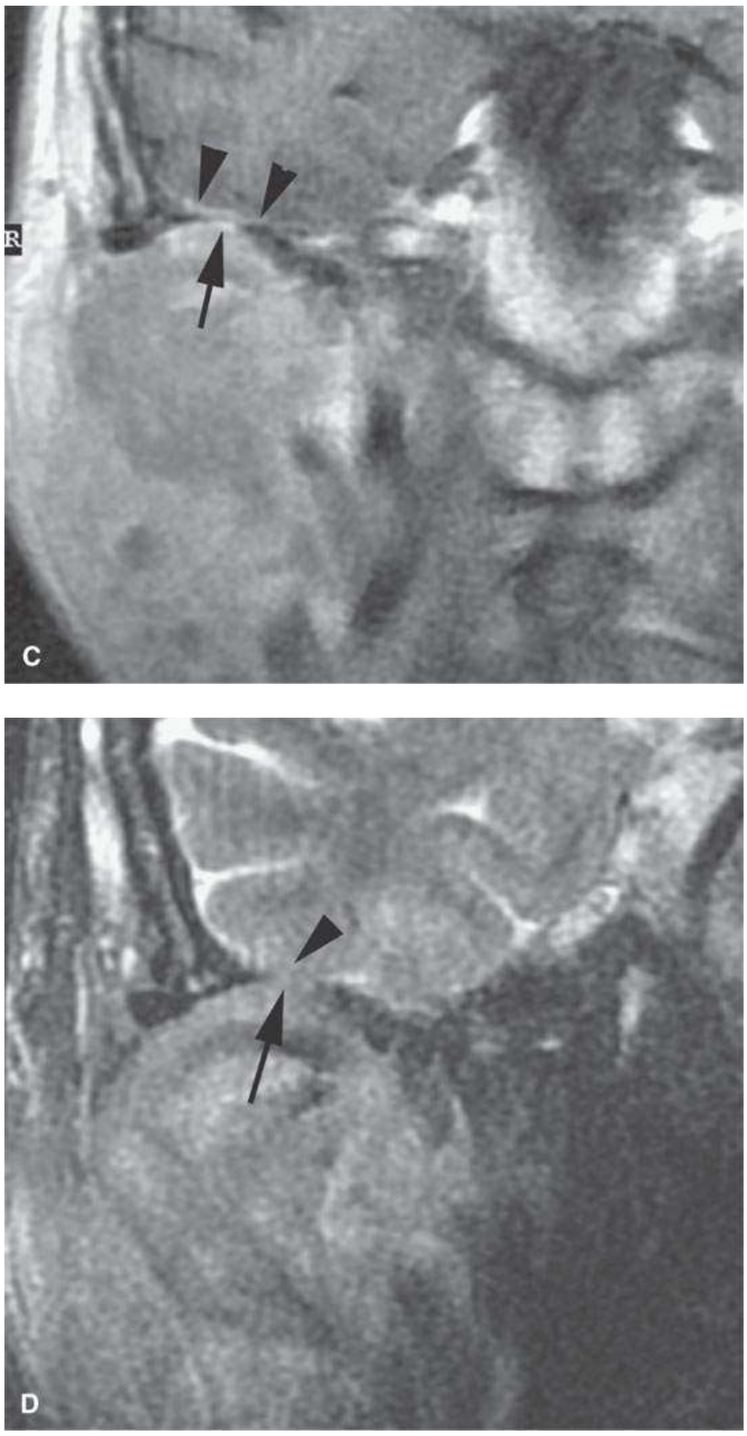

FIGURE 24.21. Magnetic resonance imaging of a patient with a highly aggressive squamous cell carcinoma of the external auditory canal. The extensive deep spread of this tumor was not expected clinically. **A**: Non–contrast-enhancedT1-weighted (T1W) image spreads medially to the styloid *(arrows)* process, almost reaching the carotid artery. **B**: Contrast-enhanced T1W image growing to encase the third division of the trigeminal nerve compared to the normal side *(arrowhead)*. **C**: Contrast-enhanced T1W image shows the bone of the condylar fossa to be invaded *(arrow)* and the overlying dura reactive or invaded *(arrowheads)*. **D**: T2-weighted image shows the bone erosion *(arrow)* and possibly transdural spread *(arrowhead)*.

Bone and Cartilage Invasion

CT shows bone invasion better than MRI (Figs. 24.19–24.22). CT excludes bone invasion with a much higher degree of confidence than MRI, and highly detailed studies must be completed through the primary site when tumor approaches bone and/or feels fixed on physical examination. MRI may show the spread of tumor within the marrow spaces of bone more graphically than CT. Spread across the skull base and calvarium to dura is better demonstrated by MRI than CT (Fig. 24.21C,D). Very high resolution MR can be used to assess invasion of the nasal and ear cartilages.

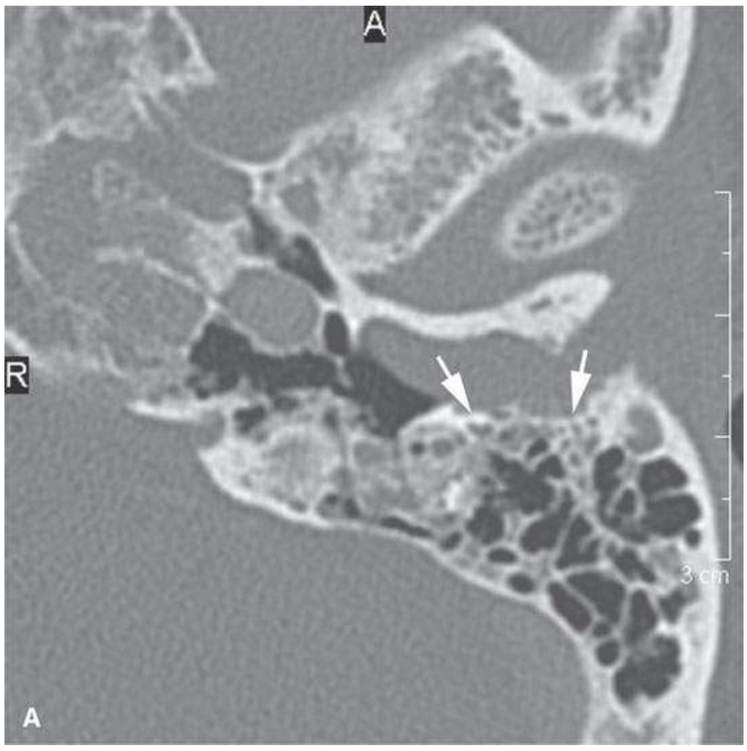
A
R
3 cm
A

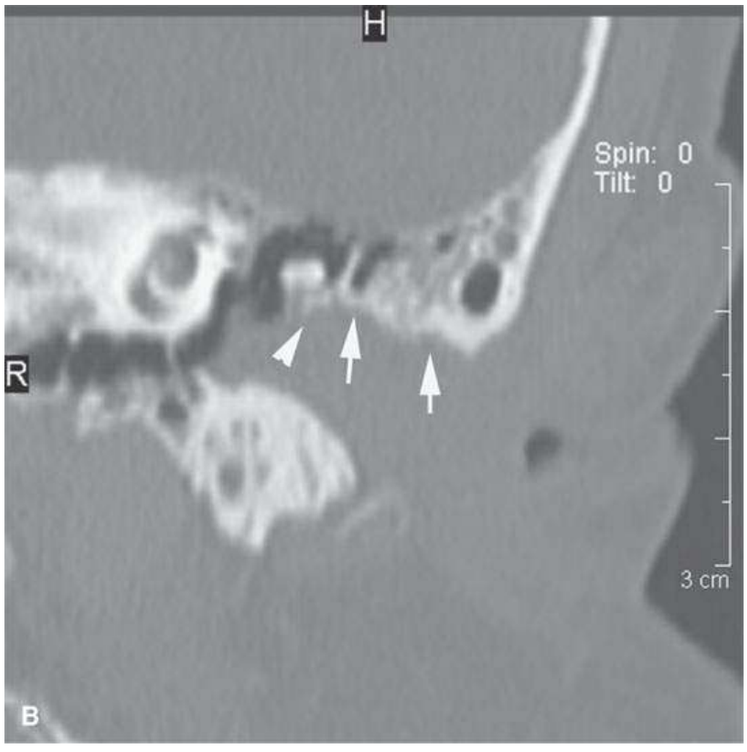
H
Spin: 0
Tilt: 0
R
3 cm
B

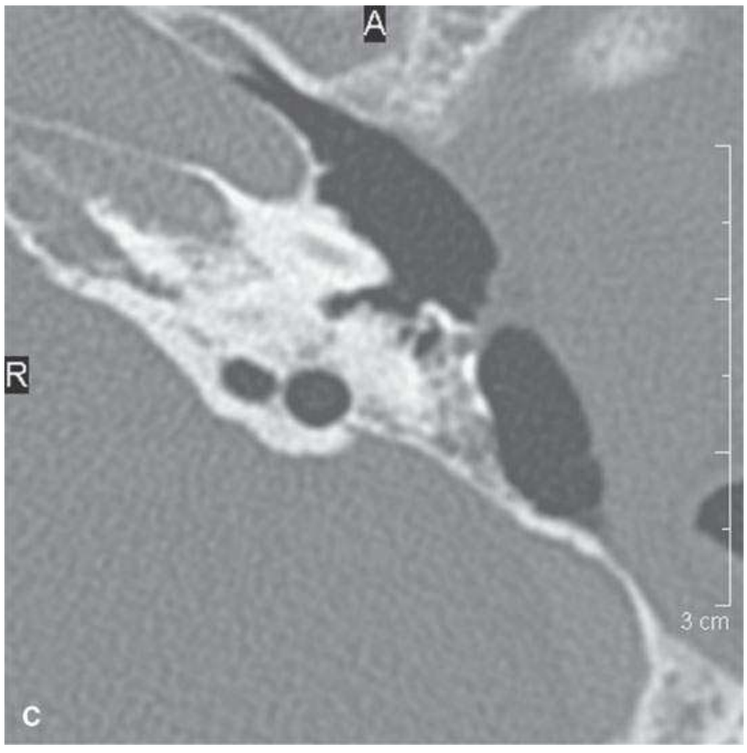
A
R
3 cm
C

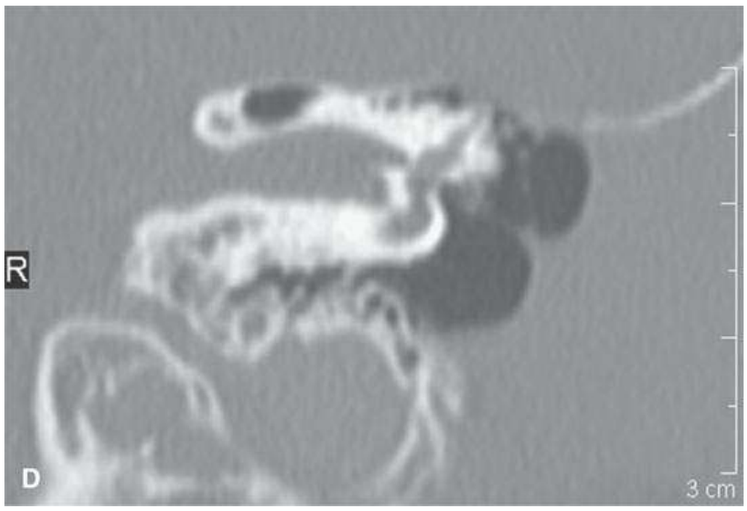

FIGURE 24.22. Computed tomography of a patient with a low-grade squamous cell carcinoma of the external auditory canal.**A, B:** Chronic bone erosion *(arrows)* and tumor confined lateral to the tympanic membrane, making a lateral temporal bone resection adequate for treatment. **C, D:** The patient status post lateral temporal resection that controlled the tumor.

Lymph Node Staging

CT and MRI may be used for evaluating the presence and extent of parotid, facial, and cervical adenopathy (Figs. 24.10–24.14); however, anatomic imaging is only adjunctive to medical decision making, which should be based on standards of treatment related to known tumor spread patterns and other mitigating risk factors. Ultrasound is used by some groups for detecting and sampling parotid and cervical nodal metastases but is not used routinely. In melanoma, FDG-PET and sentinel node techniques are a potentially more useful adjunct to surgical planning for nodal metastatic disease. These studies may also be used for Merkel cell carcinoma and occasionally SCCA.

Perineural Spread

CT and MRI can detect perineural spread (Figs. 24.1–24.9). Findings may be subtle on either examination. CT can be used for screening, but MRI is the definitive examination for establishing the extent of detectable disease and most confidently confirming that, if present, the perineural disease is only microscopic (Fig. 24.19). A systematic search of the most peripheral ramifications of the trigeminal and facial nerve to the brain stem is required (Figs. 21.50–21.52 and 24.1–24.9). If tumor fails to enlarge the nerve and/or cause it to enhance abnormally, microscopic spread remains possible. Enlargement and enhancement of inflamed nerves can mimic tumoral involvement. A rich vascular plexus accompanies the cranial nerves as they near and course through their exit foramina and often beyond. Such normal perineural enhancement must not be misdiagnosed as an abnormality possibly due to perineural tumor.

Evaluation of Recurrent Disease

Recurrent carcinoma of the skin may spread much deeper than can be appreciated on physical examination (Fig. 24.23) and is often perineural (Fig. 24.24). If the physical examination suggests deep spread, MRI and/or CT are indicated. When such deep spread is present, the bone invasion, perineural spread, and adenopathy rates increase.

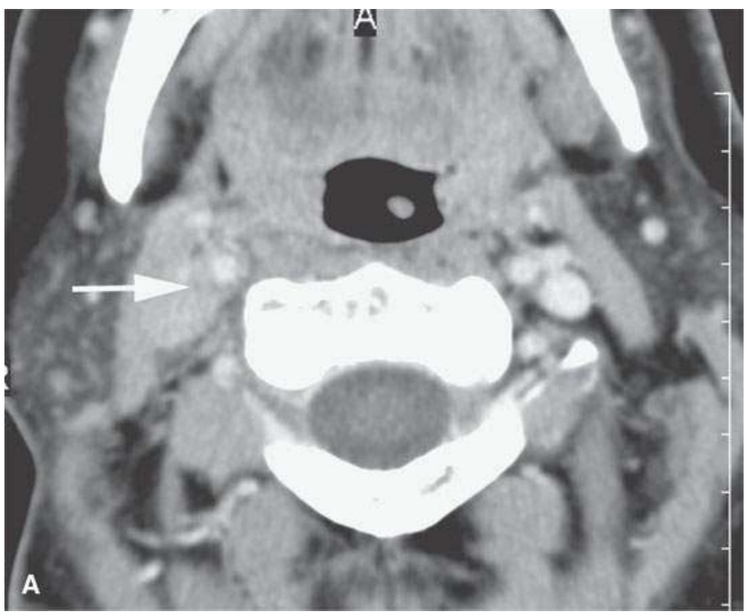

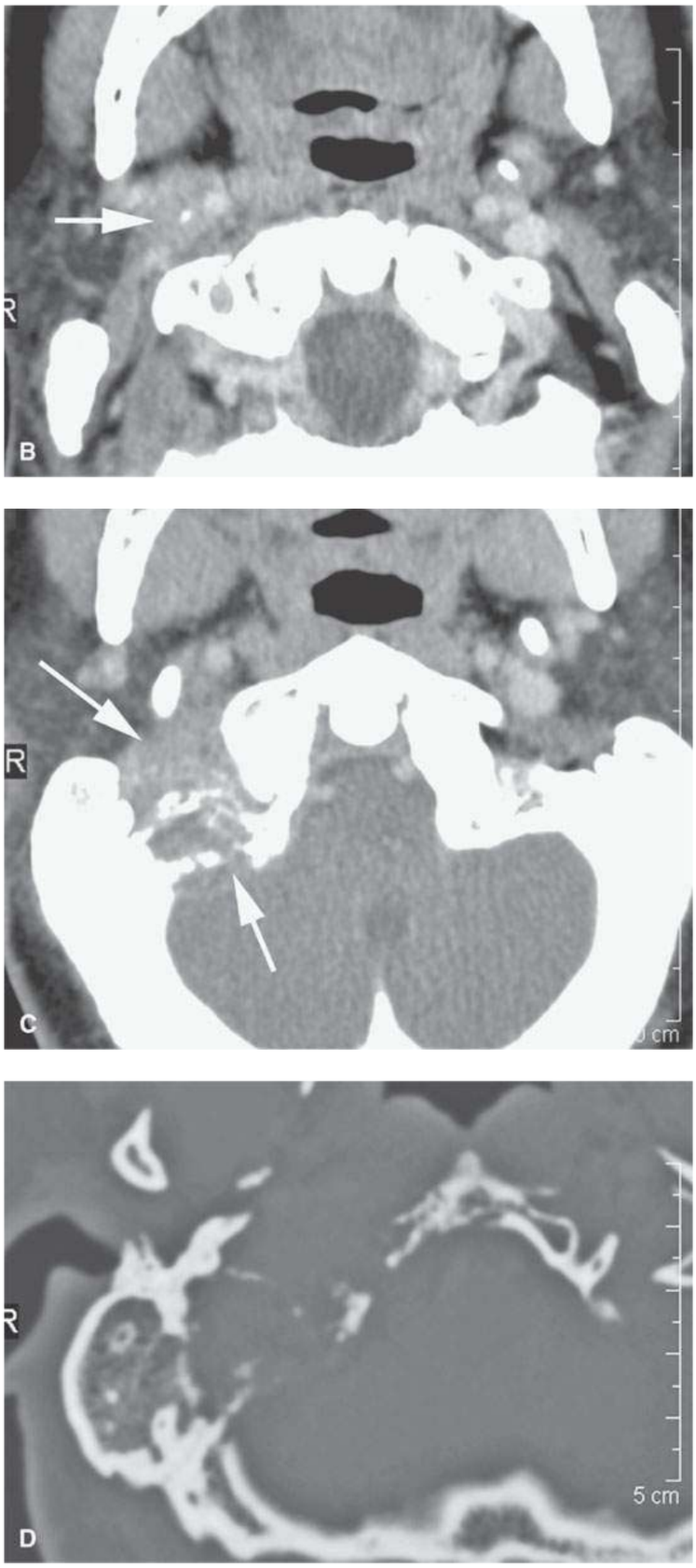

FIGURE 24.23. Contrast-enhanced computed tomography in a patient thought to have a just localized superficial failure in the skin of the neck at the original site of the squamous cell skin carcinoma; however, the patient had worsening right suboccipital headaches and otalgia**.**Deeply recurrent tumor tracks along the carotid sheath in the retrostyloid parapharyngeal space *(arrows)* are seen in **(A)** through **(C)** to eventually invade the skull base **(D).**

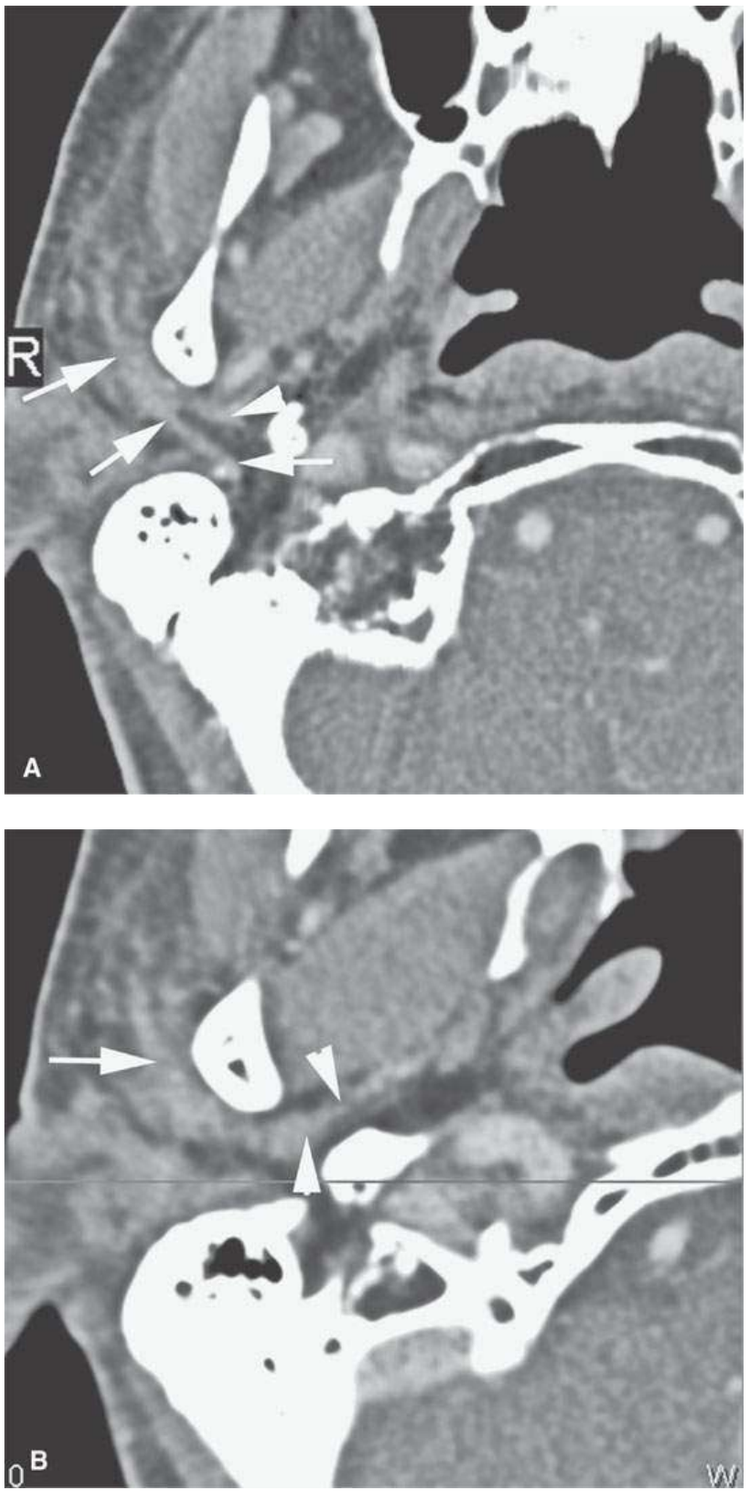

FIGURE 24.24. Contrast-enhanced computed tomography in a patient thought to have a much localized superficial failure in the skin of the periauricular region at the original site of the squamous cell skin carcinoma; however, the patient had worsening right otalgia.Deeply recurrent tumor tracks along the facial nerve *(arrows **in A and B**)* to the auriculotemporal nerve junction with V3 (*arrowheads* in A and B).

GENERAL IMAGING APPROACH

CT or MRI must be customized based on the site of primary origin. There must be highly focused images through the primary site.

Protocols should vary based on the several general regions of origin of these lesions, including the scalp, midface, perimandibular region and lower face, periauricular and periparotid region, and neck.

High-quality axial and coronal images must be available to evaluate for perineural spread, as specified in the protocols in Appendixes A and B. If CT is chosen, the initial data acquisition must be of sufficient detail to allow definitive multiplanar reformations (MPR).

Spread to nodes must account for the possibility of spread to lesser known groups that could be cut out of the images, such as those in the occipital and upper posterior neck region.

Imaging-directed needle biopsy can be used to sample disease in areas not reachable by other means. CT is usually used for guidance. Ultrasound may be used in some cases when the suspected focus is more superficial.9

LIMITATIONS OF IMAGING FINDINGS IN SURGICAL PLANNING

CT or MRI cannot distinguish soft tissue swelling and infiltration due to lymphatic obstruction and reactive peritumoral edema, the effects of a recent biopsy, infection, or prior treatment. Areas of swelling that are visible on imaging must be presumed to be involved with tumor unless an alternative explanation seems more reasonable, such as a recent biopsy.

Tumor adjacent to bone may or may not be invading the periosteum. If careful imaging with CT shows no cortical erosion or periosteal reaction, the surgical plan can be to take the periosteum as a margin; however, this lack of invasion observation must be confirmed at surgery. Bone may be remodeled adjacent to tumor

indicting at least periosteal invasion or adherence to periosteum even if no frank erosion is visible (Figs. 24.19, 24.20C, and 24.22 A,B).

Cancer invading the skull may fill the diploic space and displace dura and produce a reactive enhancement. Such spread may have invaded or only be adherent to the dura (Fig. 24.21). Irregular dural thickening suggests tumor invasion (Figs. 24.9 and 24.21C,D). Leptomeningeal or brain invasion are the most clear imaging signs of transdural spread (Fig. 24.9C–E). Imaging should only be considered suggestive of these circumstances, and the surgeon is forewarned of "probable" dural involvement. Intraoperative confirmation is required to assure the best approach to resection and closure of the area of skull and dural involvement. This is similar to the approach just suggested for periosteal and bone invasion.

Lymph nodes are better evaluated with CT than MRI because focal metastatic deposits within the nodes can generally be seen with greater clarity (Figs. 24.10–24.13) on CT, as discussed in Chapter 157. In the absence of such visible metastatic deposits, MRI and CT are dependent on size criteria for the detection of nodal metastatic disease. The accuracy of size criteria is not good enough for serious medical decision making.6

FDG-PET can improve the rate of detection of subclinical nodal metastases in SCCA, melanoma, and likely Merkel cell cancer.10 Its effect on outcome or modifying treatment plans or affecting outcomes remains unproven. It should only be used very selectively.

Sentinel node imaging can also help improve the approach to neck treatment making up for some of the deficits of anatomic imaging.

TREATMENT

Primary Site
Surgical and Medical

Skin cancer can be treated with topical chemotherapy; various minimally invasive surgical techniques; and, for more advanced lesions, wide local incision with repair of the operative defect.11,12–13

Radiation Therapy

Radiation therapy is used to limit the functional or cosmetic results that might occur from surgery. Large lesions that are generally not suitable for surgical treatment and patients medically unable to undergo an operative procedure are also treated with radiation therapy.

There is a limited, if any, role for systemic chemotherapy.

The factors used for determining treatment strategy that might be impacted by imaging include anatomic location; size; and invasion of contiguous structures, especially bone invasion.

Other factors that might influence strategy include whether the lesion is recurrent and the general medical condition of the patient as well as potential functional and cosmetic losses.

Lesions favorable for cure are ≤2 to 3 cm, those that are slow growing, and well-differentiated tumors with discrete borders that show little or no deep infiltration. Favorable lesions should not be attached to contiguous structures or involve the ear, periorbital fascia, or nose. Such cancers are well managed by the least morbid surgical procedure possible. Radiation therapy is used in selected cases where surgery might produce a suboptimal result.

Lesions unfavorable for cure include those that grow rapidly, with an infiltrating margin and that become fixed to underlying structures. Tumors involving the ear, orbital periosteum, bone, or cartilage are also unfavorable. Bone and cartilage involvement, however, are not absolute contraindications to radiation therapy. Perineural invasion has a negative impact on prognosis related to the bulk of disease and extent of spread proximally. Those with perineural spread and recurrent lesions are less likely to be cured.

Small, superficial lesions of the scalp are usually treated with surgery. More advanced lesions may require removal of the subjacent periosteum and calvarium or dura. Imaging with CT and MRI is critical to treatment planning in lesions requiring resection including the periosteum and beyond.

Regional Lymph Node Metastasis

Skin cancer patterns of region adenopathy differ from those of mucosal sites. This results in more tailored strategies to treat nodes electively or when one or more groups are involved. The parotid nodes are the most well known of the groups at risk; however, treatment plans and diagnostic strategy must account for possible spread to facial and posterior neck nodes as well.

Parotid Region and Other Lymph Node Metastasis

The lymphatic tissue within the parotid gland is in close proximity to the facial nerve. Anatomic study shows that parotid lymphatic tissue lies predominantly along the retromandibular vein. The facial nerve typically is lateral to this main vascular bundle in the parotid; thus, removal of glandular tissue lateral to the vein removes the lymphatic tissue, while dissection just lateral to and along the nerve would have a significant amount of lymphatic tissue in most patients. However, dissecting medial to the nerve might put the nerve at more risk than necessary.

Contrast-enhanced CT or MRI may be used to customize parotid resection when there are clinically positive parotid region lymph nodes. This is done to assure clearance of nodal metastases while placing the facial nerve at least risk.

In general, if imaging and physical examination show small, mobile positive nodes lateral to the expected position of the nerve, they may be removed by dissection lateral to the nerve, removing the superficial portion of the gland (Fig. 24.11C,D). More extensive spread to the skin or deep spread shown by imaging to involve the facial nerve, masseter muscle, mandible, or deep lobe of the parotid gland require a customized surgical approach that assures gross total resection (Fig. 24.12A,B). Imaging is critical in evaluating such spread. Radiation therapy will usually be added postoperatively in such advanced disease.

Elective treatment of clinically and imaging-negative parotid nodes with surgery is not used in SCCA but may be done for malignant melanoma. Primary cancer invading the parotid gland or nearby might require parotidectomy and removal of the parotid nodes.

Clinically or imaging positive nodes in the neck usually prompt neck dissection. This may be avoided by sampling upper neck nodes or relying on negative imaging to exclude all but very low volume or micrometastases. The neck can then be incorporated into the postoperative radiation therapy plan.

Occipital lymph node metastases are removed by a posterolateral neck dissection.11 Mastoid nodes are removed by a suitable regional dissection. In both cases, an ipsilateral modified neck dissection is usually added.

Facial nodes are at risk and depending on the primary site some of these facial nodes must be included in the treatment plan.

COMPLICATIONS OF THERAPY

Patients with obvious bone invasion and destruction are usually relatively asymptomatic and remain that way throughout therapy. Osteoradionecrosis of the calvarium can occur. Cerebral radionecrosis after radiation therapy for scalp cancer is rare, and it may also occur in patients treated aggressively for gross

perineural spread.14 When the parotid and temporal regions are irradiated, long-term serous otitis media may be present on CT and MRI. Bone exposures and osteonecrosis may occur and be slowly progressive.

Suggested Readings

Tart RP, Kotzur IM, Mancuso AA, et al. CT and MR imaging of the buccal space and buccal space masses. *Radiographics*. 1995;15:531–550.

Veness MJ, Porceddu S, Palme CE, et al. Cutaneous head and neck squamous cell carcinoma metastatic to parotid and cervical lymph nodes. *Head Neck*. 2007;29:621–631.

References

1. Veness MJ, Porceddu S, Palme CE, et al. Cutaneous head and neck squamous cell carcinoma metastatic to parotid and cervical lymph nodes. *Head & nNeck*. 2007;29:621–631.

2. Pitman KT, Johnson JT. Skin metastases from head and neck squamous cell carcinoma: Incidence and impact. *Head & nNeck*. 1999;21:560–565.

3. Williams LS, Mancuso AA, Mendenhall WM. Perineural spread of cutaneous squamous and basal cell carcinoma: CT and MR detection and its impact on patient management and prognosis. *Int J Radiat Oncol Biol Phys*. 2001;49:1061–1069.

4. Lin D, Franc BL, Kashani-Sabet M, et al. Lymphatic drainage patterns of head and neck cutaneous melanoma observed on lymphoscintigraphy and sentinel lymph node biopsy. *Head & nNeck*. 2006;28:249–255.

5. Chang DT, Mancuso AA, Riggs CE Jr, et al. Merkel cell carcinoma of the skin with leptomeningeal metastases. *Am J Otolaryngol*. 2005;26:210–213.

6. Galloway TJ, Morris CG, Mancuso AA, et al. Impact of radiographic findings on prognosis for skin carcinoma with clinical perineural invasion. *Cancer*. 2005;103:1254–1257.

7. Curtin HD, Ishwaran H, Mancuso AA, et al. Comparison of CT and MR imaging in staging of neck metastases. *Radiology*. 1998;207:123–130.

8. Mendenhall WM, Mancuso AA, Parsons JT, et al. Diagnostic evaluation of squamous cell carcinoma metastatic to cervical lymph nodes from an unknown head and neck primary site. *Head & nNeck*. 1998;20:739–744.

9. Miyashita T, Tateno A, Horiuchi J, et al. Short-time ultrasound of head and neck squamous cell carcinoma under radiotherapy. *J Ultrasound Med bBiol*. 2001;27:13–19.

10. Wong WL, Chevretton EB, McGurk M, et al. A prospective study of PET-FDG imaging for the assessment of head and neck squamous cell carcinoma. *Clinical otolaryngology and allied sciencesClin Otolaryngol Allied Sci*. 1997;22:209–214.

11. Liauw SL, Mancuso AA, Morris CG, et al. Definitive radiotherapy for head-and-neck cancer with radiographically positive retropharyngeal nodes: Incomplete radiographic response does not necessarily indicate failure. *Int J Radiat Oncol Biol Phys*. 2006;66:1017–1021.

12. Liauw SL, Mancuso AA, Amdur RJ, et al. Postradiotherapy neck dissection for lymph node-positive head and neck cancer: The use of computed tomography to manage the neck. *J Clin Oncol*. 2006;24:1421–1427.

13. Dhiwakar M, Khan NA, McClymont LG. Surgery for head and neck skin tumors in the elderly. *Head & nNeck*. 2007;29:851–856.

14. Koot RW, Stalpers LJ, Aronica E, et al. Cerebral necrosis after 25Gy radiotherapy in childhood followed 28 years later by 54Gy radiotherapy. *Clin Neurol Neurosurg*. 2007;109:607–612, Epub 2007 Jun 6.

Related Posts:

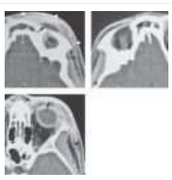
Preseptal Compartment:

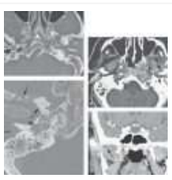
Necrotizing ("Malignant") Otitis

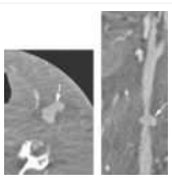
Cervicothoracic Junction: Brachial

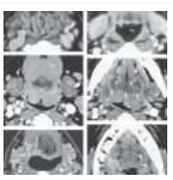
Oropharynx: Introduction

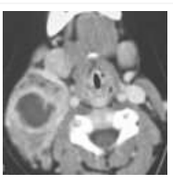
Branchial Apparatus

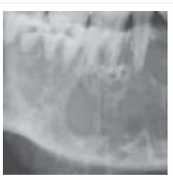
Mandible and Maxilla:

May 14, 2017 | Posted by admin in HEAD & NECK IMAGING | Comments Off